PM$_{10}$ SOURCE COMPOSITION LIBRARY
FOR THE SOUTH COAST AIR BASIN

VOLUME I

SOURCE PROFILE DEVELOPMENT DOCUMENTATION

FINAL REPORT

Prepared for

South Coast Air Quality Management District
9150 Flair Drive
El Monte, CA 91731

Project Officer: Arthur Davidson

Prepared by

J.A. Cooper,
D.C. Redline,
J.R. Sherman,
L.M. Valdovinos,
W.L. Pollard,
L.C. Scavone
and
C. Badgett-West

NEA, Inc.
10950 S.W. 5th Street, Suite 380
Beaverton, OR 97005

Disclaimer

The statements and conclusions in this report are those of
the authors and not necessarily those of the South Coast Air
Quality Management District. The mention of commercial products,
their source or their use in connection with material reported herein
is not to be construed as either an actual or an implied endorsement
of such products.

PREFACE

The South Coast Air Quality Management District (SCAQMD) is responsible for air quality in the South Coast Air Basin (SCAB) and operates a number of ambient sampling sites to monitor compliance with state and federal ambient air quality standards. The District recently initiated a PM_{10} source apportionment program which includes the use of chemical mass balance (CMB) receptor methods to establish a quantitative source impact data base which can be used to develop a state implementation plan.

The accuracy of the CMB method, however, is limited primarily by the accuracy and relevance of available source profiles. Although there have been numerous emission inventory and source characterization studies dealing with sources in the SCAB (1-17), few of the results are applicable to the current SCAQMD's CMB study. The application of these earlier results is limited for a variety of reasons such as having little chemical data or not having measured key chemical species, as well as not having collected samples in size fractions applicable to current ambient samplers or not having taken into account atmospheric modifications such as condensation. Source profile libraries are available (18,19), but they were developed for sources in other airsheds and the systematic uncertainties associated with their use in the SCAB are not only unknown but expected to be significant.

The SCAB is large and includes portions of Los Angeles, Orange, Riverside, and San Bernardino counties in southern California. It extends from the western tip of Los Angeles County, 130 miles east into San Bernardino County, and 65 miles north from its most southern point in Orange County. The Basin encompasses almost 7000 square miles, eleven million inhabitants, and about eight million on-road vehicles.

The objective of this study was to develop a source profile library for the SCAB that represents the highest priority sources and more than 90% of the emission inventory.

The first phase included the development of an experimental plan which defined the highest priority sources and species, as well as the methods that should be used to effectively utilize available resources and still meet the program needs of the SCAQMD (20).

This source profile development plan was submitted to the SCAQMD at the beginning of this study (20). Based on emissions inventory, site inspection, and preliminary receptor modeling, the highest priority sources at all monitoring sites were identified as follows:

- on-road motor vehicles

- entrained soil and road dust, and

- construction and demolition.

The relative priority of other sources, however, were substantially different at individual monitoring sites. Most of the petroleum refineries, for example, are located within a few miles of the Long Beach monitoring site, while there are no refineries within 30 or 40 miles of the Riverside site. On the other hand, farm operations, mineral processing, and unpaved road emissions are more prevalent in the vicinity of the Riverside monitoring site. There are more utility boilers in the areas surrounding the two sites near the coast (Hawthorne and Long Beach). Marine aerosol impacts will also be highest at these two sites. Emissions in the vicinity of the Hawthorne site are unusual in that they include the Los Angeles International Airport and the largest petroleum refinery, both of which are only about a mile from the site and upwind almost 50% of the time. The area round the downtown Los Angeles site includes both a major bus terminal and a major train depot. Further details on the Basin and regional features of the particulate emissions inventory and

chemical emission inventory, as well as significant features of potential local sources and high priority fugitive dust sources are identified in this earlier report (20).

Based on these source priorities and available resources, an experimental plan to develop source profiles for these sources was developed that included characterization of vehicle exhaust, vehicle profile evaluation with tunnel aerosol measurements, and direct profile measurements of entrained soil and road dust, fluid catalytic **crackers** ~~converters~~, construction and demolition, coke calciner, and rock crusher. Source profiles for the remaining sources were to be developed from values previously reported in the literature. Inclusion of the coke calciner and rock crusher in the group of sources requiring sample collection was based on special interest of the SCAQMD. The details of this experimental plan are presented in the final report for this first phase (20).

The primary objective of this current report is to provide experimental documentation for the source profiles developed as part of this study, and present the source profile library and user's guide.

The report is divided into three volumes. Volume 1 provides documentation of the experimental methods and a discussion of the results. Part I of this first volume is devoted entirely to motor vehicle emissions, while Part II discusses the methods and results for the other sources characterized as part of this study.

Volume II is the hard copy of the source profile library. It is a self contained document that includes a user guide to the library tables and profiles, a guide to the library software which is located in a pocket at the back of the volume and the source composition tables and profiles.

Volume III consists of miscellaneous appendices relevant to the discussion presented in Volume I.

ACKNOWLEDGEMENTS

TABLE OF CONTENTS

TABLE OF CONTENTS
-Continued-

VOLUME II - COMPILATION OF SOURCE PROFILE LIBRARY

VOLUME III - APPENDICES

PART I

MOTOR VEHICLE EMISSIONS

EXECUTIVE SUMMARY

The South Coast Air Quality Management District (SCAQMD)
recently initiated a PM_{10} source apportionment program which
includes the use of chemical mass balance receptor methods. The
accuracy of this method is limited primarily by the accuracy and
relevance of available source profiles. The primary objective of
this study was to develop source profiles for the highest priority
sources in the South Coast Air Basin (SCAB) and document the
development of these profiles in this report.

The highest priority source in the air basin is on-road motor
vehicle emissions, which represent one of the largest source
categories of primary particles in the South Coast Air Basin. It
also is a significant source of secondary particles, and its
emissions are primarily fine particles that have the largest impact
on health and visibility. In addition, source profiles for this
source category are poorly established in the literature and are
highly dependent on changing vehicle fleet and fuel
characteristics.

The objective of this portion of the study was to develop a
reliable source profile for vehicle emissions. The approach taken
was to develop tailpipe emission factors and source profiles for in-
use vehicles representing the SCAB vehicle fleet by using direct
tailpipe exhaust sampling methods and estimate their uncertainties
by comparing composite vehicle emission profiles developed from
laboratory studies with the results obtained from a tunnel study.
This general approach is illustrated in Figure 1. Dynamometer
tailpipe measurements and literature values were used to develop
source profiles applicable to the tunnel and the air basin. Steady
state dynamometer profiles were used to apportion the net tunnel
aerosol which was then compared to profiles developed on the basis
of tunnel vehicle miles traveled, emission factors, and source
profiles. The results of this comparison were then used to infer
the uncertainty in the composite source profile developed to
represent the entire air basin.

FIGURE 1
FLOW DIAGRAM ILLUSTRATING GENERAL APPROACH USED TO DEVELOP
A COMPOSITE VEHICLE EXHAUST PROFILE FOR THE SOUTH COAST AIR BASIN
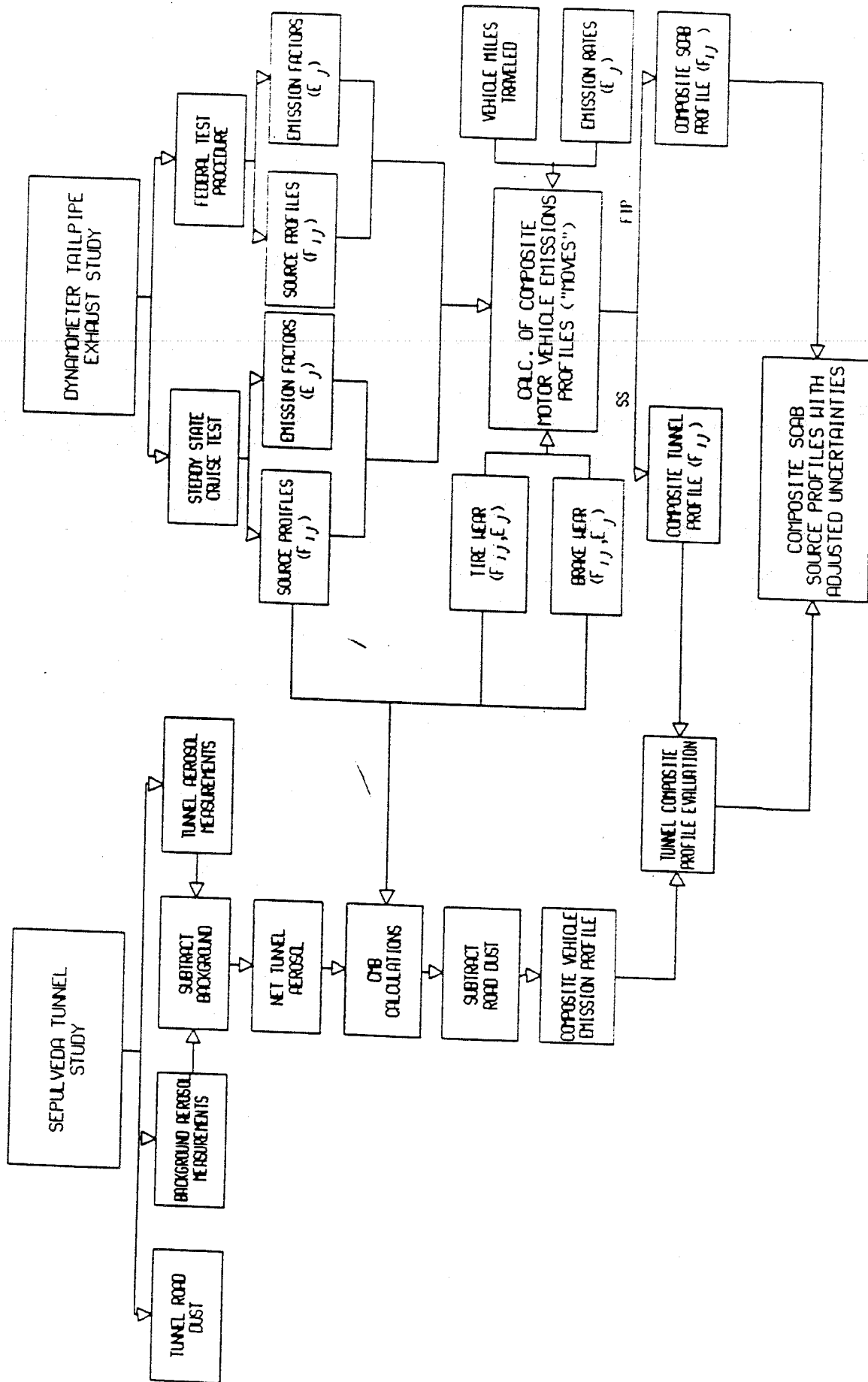
Particulate samples of vehicle exhaust from sixteen randomly selected in-use vehicles (six light duty catalyst equipped, four light duty non-catalyst equipped, four light duty diesel, and two heavy duty diesel vehicles) were collected using a dilution sampling train attached directly to the vehicle tailpipe. The emission factors and elemental content of the particulate emissions were determined for fine (< 2.5 μm), coarse (2.5-10 μm), and PM_{10} particles, as well as selected gaseous species. Source profiles and emission factors were determined for emissions during an Environmental Protection Agency Federal Test Procedure designed to represent typical driving in the South Coast Air Basin and during a special steady state test designed to simulate driving in a tunnel.

Background and Sepulveda Tunnel aerosol samples were collected simultaneously during three periods of peak traffic and the chemical composition determined. Chemical mass balance (CMB) calculations were used to determine the contribution tunnel road dust made to the tunnel aerosol which was then subtracted to determine the net vehicle generated aerosol profile.

The tunnel study results revealed that tire and brake wear emissions are much more significant than had previously been thought. In addition, emissions from semi-metal brake wear were identified as a significant new source of metallic pollution from vehicles.

Diesel exhaust was the largest source of vehicle emissions in the tunnel accounting for about 50% of the fine particle mass. Tire wear accounted for about 20% of the fine particle mass and about 30 to 40% of the coarse particle mass. Semi-metal brake wear accounted for about 5% of the fine particle mass and about 15% of the coarse particle mass. Light duty non-catalyst equipped vehicles accounted for about 13% of the fine particle mass. The contribution of catalyst equipped vehicles was not determined because it could not be resolved by the chemical mass balance method.

Emission factors were estimated from the tunnel measurements and calculated source impacts. The emission factors were generally in good agreement with the tailpipe emission factors and published literature values. A notable exception was the emission rate for light duty non-catalyst equipped vehicles using leaded gasoline which was about ten fold greater than estimated from the tailpipe emission rate and vehicle miles traveled. These results suggested that more vehicles were using leaded gasoline than indicated by the fleet characteristics.

The primary emission features of light duty non-catalyst equipped and diesel fueled vehicles were consistent with the tunnel profiles. The consistency with minor features could not be clearly evaluated because of the large contribution made by tire and brake wear components.

It was concluded that a composite exhaust profile based on Federal Test Procedure emission profiles would be representative of vehicle exhaust emissions in the air basin. The accuracy of this composite exhaust profile depends primarily on the relative emission rates and vehicle miles traveled.

It is recommended that tire and brake wear not be included in a composite vehicle profile because of large uncertainties in their emission rates and source profiles, as well as the fact that they should be resolvable as separate source categories.

It is also recommended that the source profile for both tire and brake wear emissions be determined with particular emphasis on emissions from semi-metal brakes.

LIST OF FIGURES

LIST OF TABLES

LIST OF TABLES

-Continued-

1.0 INTRODUCTION

On-road motor vehicle emissions represent one of the largest source categories of primary particles in the SCAB, a significant source of secondary particles, and its emissions are primarily fine particles which have the largest impact on health and visibility. In addition, source profiles for this source category are poorly established in the literature, and are highly dependent on changing vehicle fleet and fuel characteristics. Because of these features, the development of a reliable source profile for this category was given the highest priority (20).

Aerosol particles generated by the operation of on-road motor vehicles include resuspended road dust, tailpipe exhaust, wear products (tire, clutch, brake, road surface, etc.), and other miscellaneous emissions. Road dust, however, is not included in the on-road motor vehicle category as used in this discussion because 1) material from this source may be reintrained by wind, 2) its chemical and physical properties are similar to soil, and 3) potential methods of control are substanytially different from tailpipe emissions. Of the remaining types of aerosols generated by this source category, exhaust and tire wear emissions are the largest. Of these, only the tailpipe exhaust was characterized because of its expected large contribution, high degree of variability, and the inappropriateness of literature values.

The chemical features of on-road motor vehicle exhaust emissions depend primarily on the type of vehicle, its age, operating conditions, and the type of fuel burned. Because of the strong influence of these factors, the changing chemical characteristics of fuels, and changing fleet population, previously determined profiles for this source category are not appropriate for the South Coast Air Basin (SCAB). Much of the current vehicle emissions data in the literature were developed in field studies outside of California, did not include fine (< 2.5 μm) and PM_{10} particle size measurements and did not include all the species of current interest.

1

Emission factors and source profiles for vehicles have
generally been based on three approaches. Studies have been
conducted in laboratory controlled environments, in-use controlled
air facilities, or in source-enriched open air sites. Laboratory
measurements cover a wide range of typical urban driving patterns,
but it is difficult to test enough in-use vehicles with this
approach to adequately represent the eight million vehicles in the
SCAB. In addition, dynamometer studies measure only exhaust, do not
include wear and evaporative emissions, and are not able to simulate
the rapid, large scale mixing and dilution found on the road (21).
In-use controlled air facility studies in tunnels (22,23), for
example, obtain a better sampling of the vehicle fleet by integrat-
ing the emissions from thousands of vehicles and include evaporative
and wear emissions. The driving pattern typical of tunnels,
however, does not include driving cycles such as cold starts,
acceleration, deceleration, braking, shifting, and turning that are
typical of urban driving and known to have substantially larger
emissions rates than the steady driving typical of tunnels. In
addition, emissions during these different driving patterns are
expected to significantly exceed those of steady state tunnel
driving.

Open air measurements near roads, street canyons, and distri-
bution points for trucks and buses can provide insights into vehicle
profiles (relative chemical composition) under the prevalent driving
conditions, but cannot provide a mass balance necessary for calcu-
lating absolute emission factors.

There have been relatively few tailpipe exhaust characteriza-
tion studies in the past decade, and most of the earlier studies
measured total particulate emissions and characterized only the more
abundant species such as carbon, sulfur, lead, bromine, and
chlorine. Recent tunnel studies in the east provided profiles for
major fleet categories; i.e., diesel and gasoline fueled vehicles.

2

The results reported in the last few years were based on samples collected in the 1970's, and their value to chemical mass balance (CMB) calculations on samples collected in the SCAB in the late 1980's is limited. Although previous tunnel studies have been used to develop profiles for individual vehicle types, the tunnel characteristics required to resolve individual vehicle types are not available in the SCAB.

Thousands of tailpipe emissions tests using a chassis dynamometer are performed every year. Most of these tests, however, are conducted for regulatory purposes and measure only regulated gaseous species from gasoline fueled vehicles and particulate mass, along with the regulated gaseous species in the emissions from diesel fueled vehicles. Special studies of exhaust emissions have addressed other species (11,24-29), but have not measured all the species under the conditions required by this project and have not measured emissions from in-use vehicles that would reasonably represent the 1987 SCAB vehicle fleet.

Two sampling experiments were conducted as part of this study for the development of an on-road motor vehicle source profile: direct tailpipe exhaust measurements and tunnel measurements. Internal consistency and uncertainties were evaluated by comparing the direct tunnel measurement profile with results calculated for the vehicle mix using the tunnel samples and appropriate tailpipe profiles.

The objective of this task was to develop tailpipe emission factors and source profiles for in-use vehicles representing the SCAB vehicle fleet by using direct tailpipe exhaust sampling methods, and estimate their uncertainties by comparing composite vehicle emission profiles developed from laboratory studies with the results obtained from tunnel studies.

2.0 THEORETICAL APPROACH

2.1 Composite Vehicle Exhaust Profile

A chemical profile representing average tailpipe exhaust emissions in the SCAB is a composite of emissions from a wide range of vehicle types, ages, operating conditions, and fuel types. The fractional concentration of each chemical species in a composite air basin profile, F_{ic}, can be calculated from individual tailpipe exhaust composition profiles, F_{ij}, and a weighting ratio using the following equation:

$$F_{ic} = \sum_{j} F_{ij} \, R_j \tag{1}$$

where

$$R_j = V_j \, E_j \div \sum_{j} V_j \, E_j \tag{2}$$

and the subscript j refers to one of the vehicle type, age, operating conditions, and fuel type combinations, V_j is the vehicle miles traveled under the jth combination of conditions, and E_j is the emissions factor (mg/mile) for the jth combination of operating conditions. The product $V_j E_j$ represents the total mass of particles emitted under the jth set of conditions and the summation over all j conditions represents the total particulate emissions for this source category in the whole air basin.

A program called MOVES (Motor Vehicle Emissions Signatures) developed by NEA was used to calculate the composite motor vehicle emissions signature. A detailed description of this program is presented in Appendix A in Volume III of this report.

4

2.2 Exhaust Profiles Developed from Tunnel Measurements

Tunnels have been used to investigate aerosol chemistry of vehicle emissions and to develop emission factors and source profiles for over twenty years (22,23,24-38). The vast majority of these studies have been conducted in tunnels one mile or longer in length and located in the eastern part of the United States. Many of the methods developed for these studies and much of the data have come from studies conducted in the Allegheny and Tuscarora Tunnels of the Pennsylvania Turnpike by Pierson and co-workers (22,26-33,38) One of the primary advantages of a tunnel study is that the emissions sampled are representative of a large number of vehicles in a normal use pattern and include all sources of emissions.

The method used to develop emission factors and source profiles from tunnel measurements is based on a mass balance concept; i.e., the vehicle generated aerosol is equal to the difference between the aerosol that exits the tunnel and the aerosol that enters. This net aerosol chemistry is then related to vehicle miles from a measure of the number of vehicles and the length of the tunnel. In some cases, the emissions can be separated into vehicle type by regressing the percent vehicle composition against individual species.

This is accomplished experimentally by simultaneously sampling the air that enters and leaves a tunnel while measuring the tunnel air flow and determining the traffic count and composition.

Several types of emission factors can be calculated from tunnel data sets depending on the type of data available. The emissions rate for the ith species averaged over all vehicles during the kth sampling interval, $\overline{E}_{ik}$, is calculated from the equation:

$$\overline{E}_{ik} = \Delta_{ik} \, V_k \div T_k \qquad\qquad (1)$$

where Δ_{ik} is the ith species concentration difference ($\mu g/m^3$) between tunnel exit and incoming air, V_k is the total volume of air (m^3) through the tunnel, and T_k is the total distance driven (miles); i.e., the number of vehicles of all types multiplied by the length of the tunnel. As implied by its definition, $\bar{E}_{ik}$ is not constant and can change with each sampling interval as the characteristics of the vehicle fleet change. This emission factor is of value in other areas only to the degree that the conditions and fleet characteristics in the tunnel during the kth sampling interval are similar to the conditions and fleet characteristics in the area of interest.

Two similar equations can be written in terms of either the emissions rate for the jth vehicle category (e.g., heavy duty diesel) averaged over all emissions from that category, $\bar{E}_{ijk}$, or the emissions rates from specific source categories such as light duty vehicle tire wear, heavy duty diesel exhaust, etc., E_{ijk}:

$$\bar{E}_{ijk} = \bar{\Delta}_{ijk} \, V_k \div P_{jk} \, T_k \qquad (2)$$

and,

$$E_{ijk} = \Delta_{ijk} \, V_k \div P_{jk} \, T_k \qquad (3)$$

where $\bar{\Delta}_{ijk}$ is the average mass difference for the ith species associated with the jth vehicle category, Δ_{ijk} is the mass difference associated with the jth source and P_{jk} is the fraction of vehicles in the jth category ($\sum_j P_{jk} = 1$). Emissions factors for specific vehicle categories cannot be calculated directly from tunnel data since $\bar{\Delta}_{ijk}$ and Δ_{ijk} are not measured.

Most probable source-specific emission factors, however, can be estimated by one of two methods; analysis of variability or use of a chemical mass balance approach.

Variability analysis has been used extensively by Pierson and co-workers in their investigations where traffic could be separated

into two main vehicle categories, light duty gasoline fueled
vehicles and heavy duty diesel vehicles. For this two component
case, a general emission factor equation can be written as:

$$E_k = \sum_j \overline{E}_{jk} P_{jk} \qquad (4)$$

and simplified to:

$$\overline{E}_k = E_{1k} P_{1k} + E_{2k} P_{2k} \qquad (5)$$

and

$$P_{1k} + P_{2k} = 1 \qquad (6)$$

Combining equations 5 and 6 and rearranging the terms yields the
following equation:

$$\overline{E}_k = P_{1k} (\overline{E}_{1k} - \overline{E}_{2k}) + \overline{E}_{2k} \qquad (7)$$

Since this is a linear equation in P_1, a plot of $\overline{E}$ vs. P_1 will yield
intercepts at $\overline{E} - \overline{E}_1$, and $\overline{E} - \overline{E}_2$. Thus, the emission rate for two
main vehicle categories such as heavy duty diesel trucks and light
duty gasoline vehicles can be resolved by a linear least-squares
regression.

This approach worked well for the Pennsylvania Turnpike tunnels
in the 1970's where the traffic was easily separated into light duty
gasoline vehicles and heavy duty trucks, and where the fraction of
heavy duty diesel vehicles ranged between 7% and 75% of the vehicles
using the tunnels (32).

The other approach to calculating individual vehicle emissions
factors is to use a chemical mass balance approach. In this case,
it is assumed that the tunnel concentration difference is due to the
sources of emissions in the tunnel, i.e.,

$$\Delta_{ik} = \sum_j F_{ij} M_{jk} \qquad (8)$$

where F_{ij} is the source profile for the jth source (fractional
concentration of the ith species in emissions from the jth source)

and M_{jk} is the total mass ($\mu g/m^3$) contributed to the tunnel aerosol from the jth source during the kth measurement interval.

Equation 8 can be solved for M_{jk} using the steady state source profiles developed in the first part of this project. The vehicle specific emissions factors can then be calculated using Equations 2 or 3 by substituting M_{jk} for either Δ_{ijk} or $\overline{\Delta}_{ijk}$ depending on whether F_{ij} represents the fractional composition for all the emissions from a single vehicle category or a single component such as exhaust.

2.3 Estimating Source Profile Uncertainties

The general approach used to estimate uncertainties for the composite SCAB vehicle emissions source profiles is illustrated in Figure 1. Composite vehicular source profiles were developed for steady state conditions typical of the Sepulveda Tunnel and for the SCAB using the Federal Test Procedures (FTP) to represent driving conditions in the Air Basin. The tailpipe measurements were supplemented with literature values for tire and brake wear. The steady state composite vehicle emissions were compared to the tunnel aerosol after subtracting the background and road dust aerosol. The results of this comparison were used to estimate the uncertainty of the composite source profile calculated for the Air Basin using the results from the FTP exhaust sampling.

3.0 EXPERIMENTAL METHOD

3.1 Vehicle Exhaust Sample Collection

3.1.1 Overview

Collection of vehicle exhaust samples was a cooperative project involving the California Air Resources Board (CARB), South Coast Air Quality Management District (SCAQMD), and NEA. The SCAQMD acquired the vehicles, and NEA tested the vehicles in cooperation

8

FIGURE 1

FLOW DIAGRAM ILLUSTRATING GENERAL APPROACH USED TO DEVELOP A COMPOSITE VEHICLE EXHAUST PROFILE FOR THE SOUTH COAST AIR BASIN
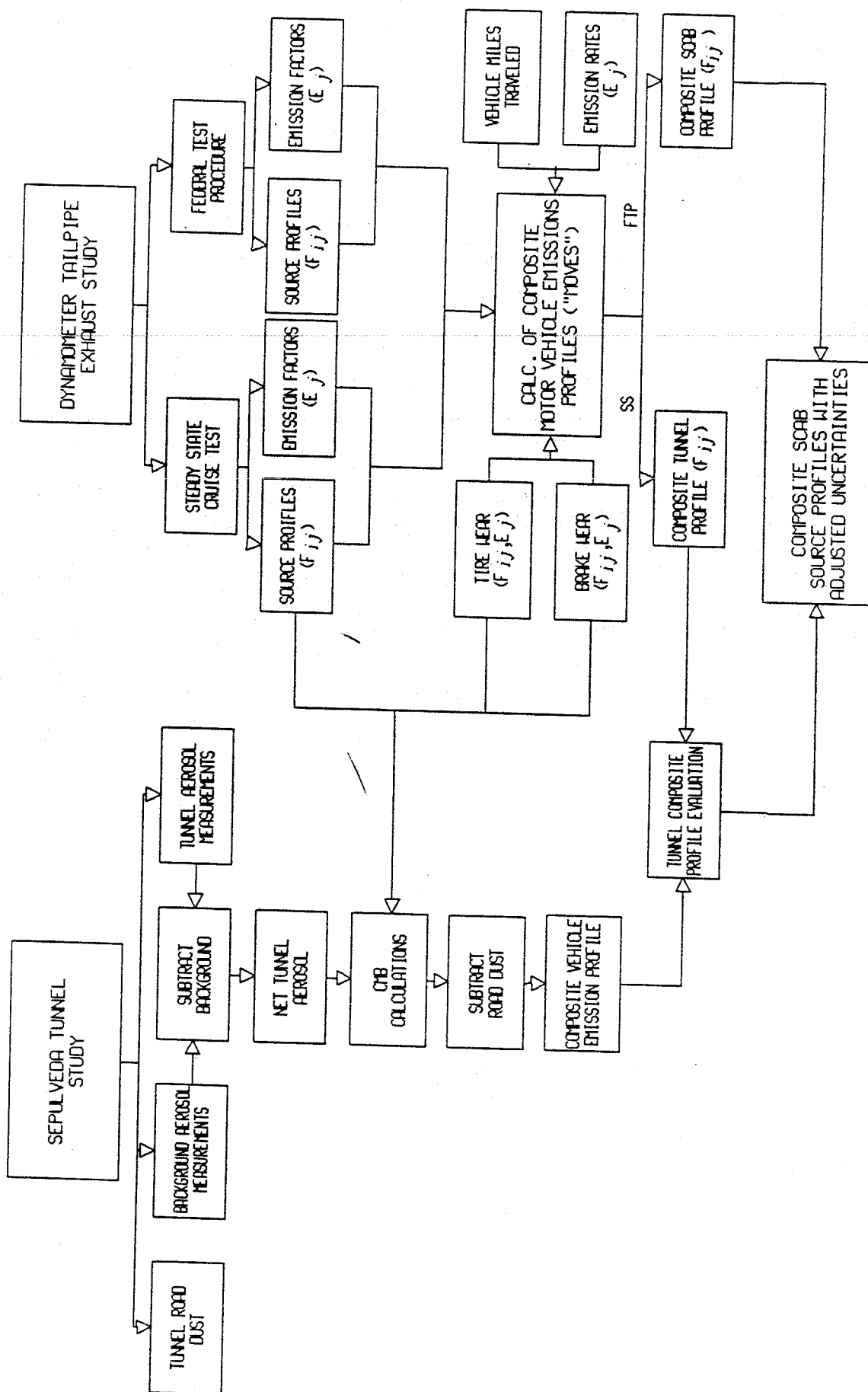
with the CARB who operated the dynamometers and constant volume sampling system (CVS) at their Haagen Smit Laboratory. Vehicles were randomly selected to represent specific vehicle fuel use categories by the SCAQMD from in-use vehicles owned and operated by employees of the SCAQMD. Selected vehicles were delivered to the Haagen Smit Laboratory the day before testing. The vehicle exhaust system was examined prior to testing and rejected if leaks were observed and could not be easily fixed. Other than this screening, all vehicles were tested in the condition they were received.

3.1.2 Characteristics of Vehicles Tested

Sixteen vehicles were tested: four light duty vehicles using leaded gasoline (LDV-L), six light duty vehicles using unleaded gasoline with catalysts (LDV-U), four light duty vehicles using diesel fuel (LDV-D), and two heavy duty vehicles using diesel fuel (HDV-D). The characteristics of these vehicles are listed in Table 1. The model year ranged from 1962 to 1986, and the odometer readings ranged from 5600 to 152,468. The LDV engine displacements ranged from 108 to 360 cubic inches, and the HDV's had 636 and 855 cubic inch displacements.

3.1.3 Particulate Sampling System

Vehicle tailpipe exhaust samples were collected from vehicles using unleaded and leaded gasoline and light and heavy duty vehicles using diesel fuel. A special dilution sampling system was attached directly to the tailpipe and between the CARB's CVS system to collect cooled and diluted particulate samples from the first three vehicle types mentioned above. A similar dilution sampler was used to collect samples from heavy duty diesel vehicles, but it was inserted downstream of the CARB's dilution chamber and upstream of their CVS system.

Table 1

CHARACTERISTICS OF VEHICLES TESTED

Vehicle No.	Make/Model	Year	Engine Size(CID)	No. Cylinders	Fuel[a] Type	Mileage
1	Chry. Reliant K	81	156	4	Unleaded (0.01)	29,874
2	Chry. Dodge Ram Van	83	318	8	Unleaded (<0.001)	49,349
3	Chry. Reliant LE	85	134	4	Unleaded (<0.001)	5,600
4	Toyota Corona	82	144	4	Unleaded (0.005)	45,388
5	GM Buick Regal	80	305	8	Unleaded (<0.001)	38,308
6	Toyota Camry	86	121	4	Unleaded (0.034)	9,328
7	Mercedes 240D	80	146	4	Diesel	83,033
8	GM Olds 98 Regency	79	350	8	Diesel	152,468
9	Mercedes 300D	77	183	5	Diesel	169,472
11	GM Olds Cutlass	80	350	8	Diesel	68,483
10	GM Chevy Nova	62	194	6	Leaded	71,830*
12	Datsun 610	73	108	4	Leaded (>0.1)	34,624
14	Chry. Dodge Van Tradesman	77	360	8	Leaded (>0.1)	28,755
15	Chry. Dodge P/U Camper	67	318	8	Leaded (>0.1)	98,659
HDD	Peterbilt Cummins 350	82	855	6	Diesel	164,476
HDD	Ford 8000 Catapillar 125	82	636	6	Diesel	

a. Numbers in parentheses are the lead content of the gasoline in the tank in grams per gallon provided by CARB. The 1968 average lead concentration in leaded gasoline was estimated to be 0.64 grams per gallon.

* Odometer miles may be off by 100,000 miles

11

The experimental arrangements are illustrated in Figures 2 and 3. Figure 2 shows a schematic of our single stage dilution sampler used to collect samples from vehicles having low emission rates such as vehicles using unleaded gasoline. The second sampling system shown in Figure 3 incorporates a secondary dilution stage which was used primarily on vehicles having high emission rates such as vehicles using diesel fuel. The location of the dilution sampler in the heavy duty diesel sampling system is illustrated in Figure 4. The first step of dilution for heavy duty diesel exhaust occurs after a portion of the exhaust is isokinetically removed from an 18 inch diameter main CARB primary residence chamber. This diverted exhaust diluted with the CARB's system, was isokinetically sampled with NEA's two stage dilution system.

Both systems were connected directly to a vehicle's exhaust tailpipe using normal CARB coupling devises. This generally consisted of a short piece of high temperature resistant flexible hose which was connected to the tailpipe with stainless steel hose clamps and to a stainless steel coupler at the other end with hose clamps. The coupler was then connected to NEA's dilution chamber with stainless steel clamps. Generally, the distance from the end of the tailpipe to the inlet of the dilution sampler was less than about one foot. This distance, however, was as much as three or four feet for a few vehicles with dual tailpipes. In this latter case, the extended tubing consisted of insulated, smooth-walled stainless steel tubing.

NEA's tailpipe exhaust dilution sampler is an all stainless steel system consisting of a dilution and mixing section, residence chamber, and a sampling chamber. The hot exhaust gas stream is introduced into the first stage dilution and mixing section through a double walled 4 inch diameter stainless steel pipe preheated to a temperature between 120° and 180°C to prevent condensation before mixing with the dilution air. In the single
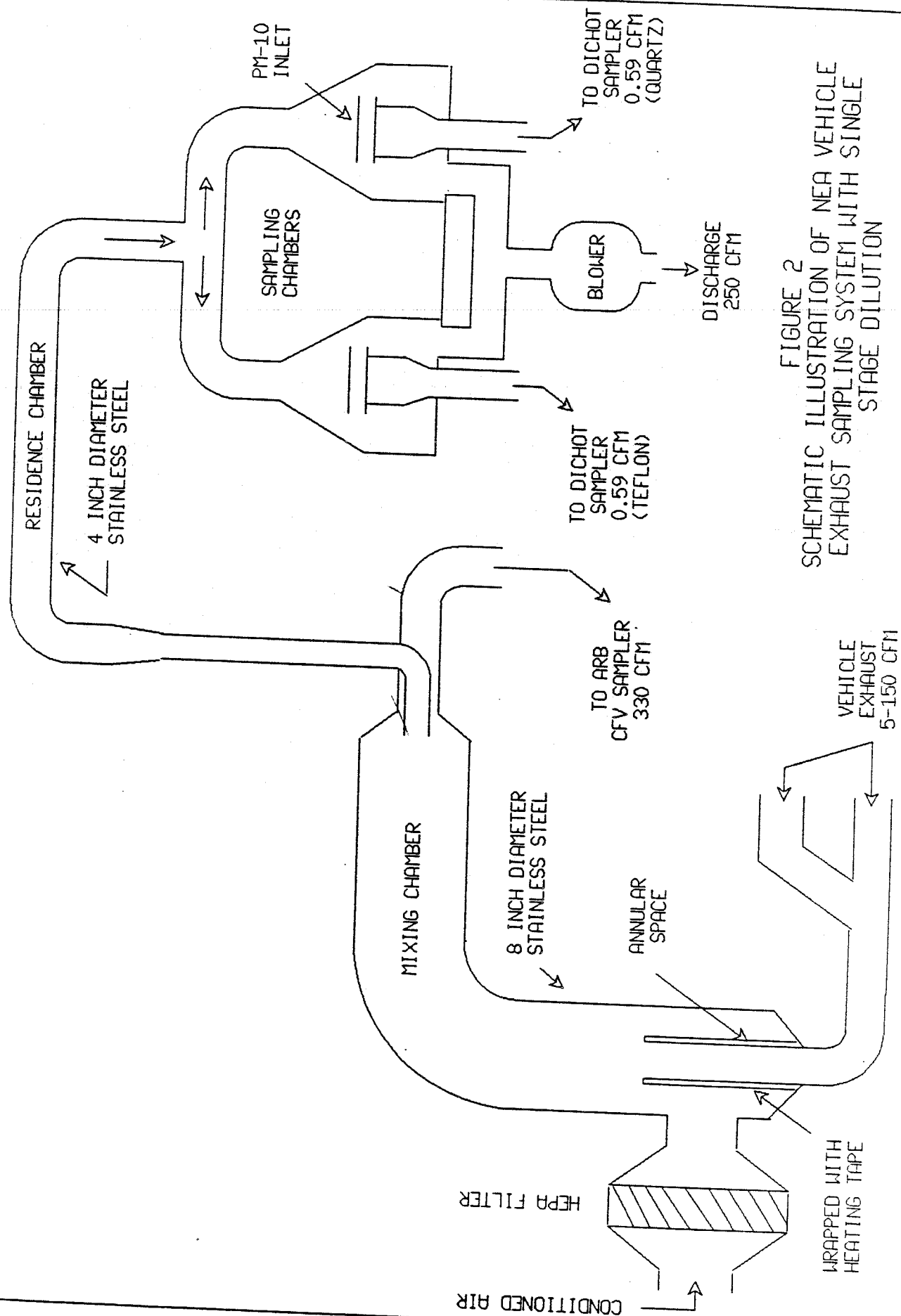
FIGURE 2
SCHEMATIC ILLUSTRATION OF NEA VEHICLE
EXHAUST SAMPLING SYSTEM WITH SINGLE
STAGE DILUTION

13

TO DICHOT SAMPLER 0.59 CFM (QUARTZ)

SAMPLING CHAMBERS

BLOWER

DISCHARGE 88-91 CFM

TO DICHOT SAMPLER 0.59 CFM (TEFLON)

RESIDENCE CHAMBER

4 INCH DIAMETER STAINLESS STEEL

TO ARB CFV SAMPLER 330 CFM

VEHICLE EXHAUST 5-150 CFM

CONDITIONED AIR 68 CFM

BLOWER

MIXING CHAMBER

8 INCH DIAMETER STAINLESS STEEL

ANNULAR SPACE

HEPA FILTER

WRAPPED WITH HEATING TAPE

AMBIENT AIR
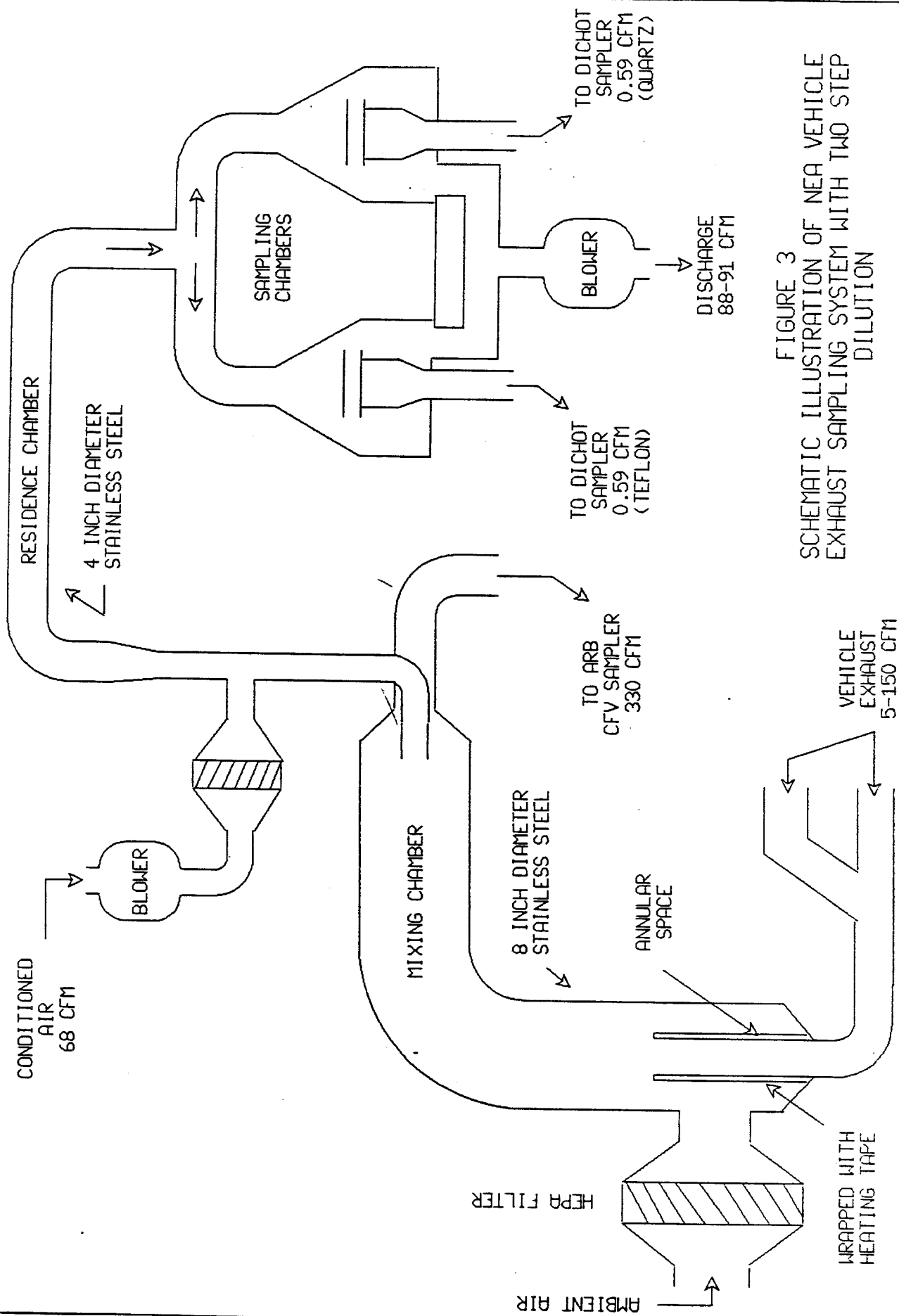
FIGURE 3

SCHEMATIC ILLUSTRATION OF NEA VEHICLE EXHAUST SAMPLING SYSTEM WITH TWO STEP DILUTION

FIGURE 4

FLOW DIAGRAM FOR HEAVY DUTY
DIESEL EXHAUST SAMPLING SYSTEM

15
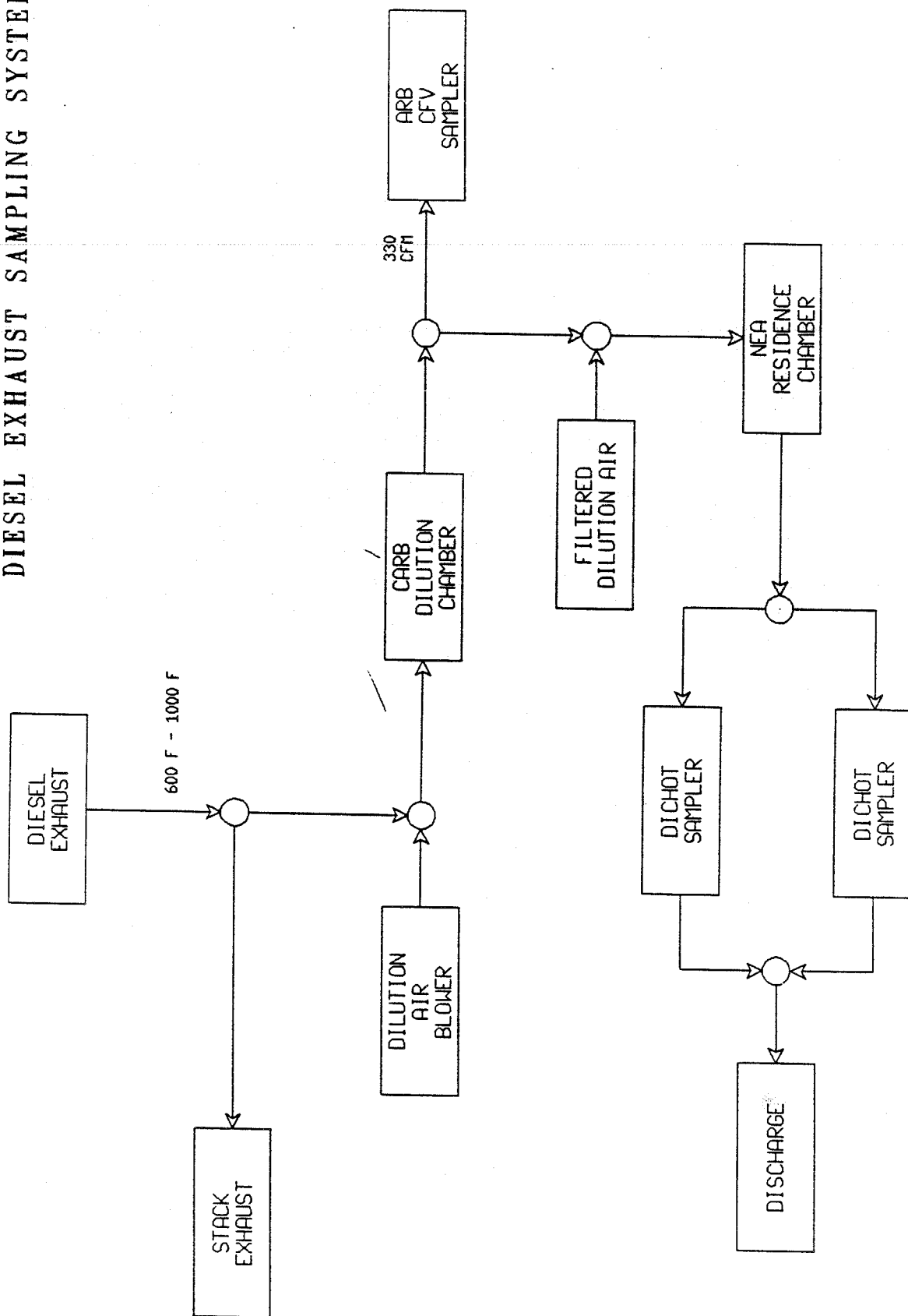
stage dilution system, cooled (10°- 15°C) dilution air was intro-
duced into the mixing chamber through a high efficiency filter with
a pressure drop less than 2 inches of water. In the two step
dilution system, ambient dilution air was used in the first stage of
dilution and conditioned dilution air was used downstream at the
second stage of dilution.

The mixing and dilution section of the system consisted
of an 8 inch diameter stainless steel pipe with a 90° elbow about
two feet from the first stage of the mixing chamber where dilution
air is added and about eight feet from the point where a fraction of
the mixed flow was extracted through a 2 inch diameter "scoop" tee
for particulate sampling. Most of the exhaust passed through this
dilution chamber to the CARB's normal CVS system where exhaust gases
were analyzed by the CARB. The small portion of the exhaust stream
extracted for particulate sampling was either further diluted with
conditioned and filtered air, or passed directly through the resi-
dence chamber to the sampling chambers where two Sierra virtual
impactors with standard 10 μm inlets collected fine and coarse
particles on Teflon and quartz fiber filters.

The single stage system was used to sample the light
duty catalytic vehicles, vehicle numbers 1-6, and two light duty
diesel vehicles, vehicle numbers 8 and 9. The remaining vehicles
were sampled using the two stage dilution sampler.

Only a small portion ($\cong$ 5%) of the primary diluted
exhaust gas stream was isokinetically diverted through the "scoop"
tee for particle sampling with the two stage dilution sampler. A
larger fraction was drawn from the mixing chamber with the single
stage sampler which resulted in the extraction of a non-isokinetic
sample in which the aspiration ratio for 10 μm particles was 0.78.
The effect of this non-isokinetic sampling was less than 1%,
however, for 2 μm diameter particles which had aspiration ratios
of 0.99. Even the larger deviation from non-isokinetic sampling for

16

10 μm particles was considered negligible because most of the coarse particulate mass is associated with particles substantially less than 10 μm.

The flow rate and temperature of the exhaust gases varied over a wide range. Exhaust flow rates ranged from 5-150 cfm and temperatures ranged between 95°C to 400°C. The highest temperatures and flow rates were associated with the larger engines being operated at the higher speeds. The temperature in the residence chamber ranged from 24°C to 49°C, with the single stage dilution sampler, and from 26°C to 34°C with the secondary dilution system.

The average residence time in the dilution and mixing chamber was 0.3 seconds for the single stage dilution sampler and 0.5 seconds for the two stage system. The total residence time before sample collection was 1.5 seconds for the single stage sampler and about 3.5 seconds for the two stage sampler.

The particle concentration measured with the dichotomous sampler (C_d) using the two stage dilution system was related to the concentration in the mixing and dilution chamber (C_t) by the dilution ratio (R)

$$C_t = C_d R$$

where

$$R = \frac{V_d + V_s}{V_s}$$

V_d = volume of secondary dilution air

V_s = volume of exhaust sample

This dilution ratio was constant during each test but ranged from about 4.0 to 4.5 between the tests. The vehicle emission rates for both particles and gases were calculated using this dilution ratio.

17

3.1.4 Vehicle Testing Procedure

Particle samples were collected during a standard EPA federal test procedure (FTP) and a steady state (SS) test in which the vehicle was operated at a constant 35 mph. The testing sequence started by storing the vehicle in a temperature controlled (68°F to 86°F) room for 13-24 hours after passing an exhaust system check. The vehicle was then pushed into the dynamometer test area and connected to the dilution sampler and CVS system. All of the dilution air flows were started prior to starting the engine. The dichotomous samplers were started simultaneously with the starting of the engines and temperature and flow rates monitored during the test.

The first test was the FTP which simulates a typical driving pattern for Los Angeles. The dichotomous samplers were turned off during the ten minute soak period of the FTP and turned on again when the engine was restarted.

After the FTP was completed, the vehicle and samplers were turned off. New filters were installed and the system prepared for a steady state test. In this test, the vehicle was started and its speed adjusted to 35 mph, with a dynamometer load equivalent to 50 mph, at inertia weight on a level road. This steady state test was intended to match the vehicle operating conditions in the tunnel.

This test sequence was followed with all the vehicles except the heavy duty diesel trucks. The CARB's heavy duty vehicle dynamometer was not capable of running a FTP. Instead, a test cycle was developed that consisted of running the vehicle through a series of accelerations, gear changes, and steady speeds. The test cycle used is illustrated in Figure 5. The procedure took the trucks through three gear changes, two accelerations, and one deceleration over a period of six minutes.

HDD TRUCK CYCLE TEST

ENGINE SPEED vs. TIME

Engine Speed (RPM)
(Thousands)

Time in Minutes
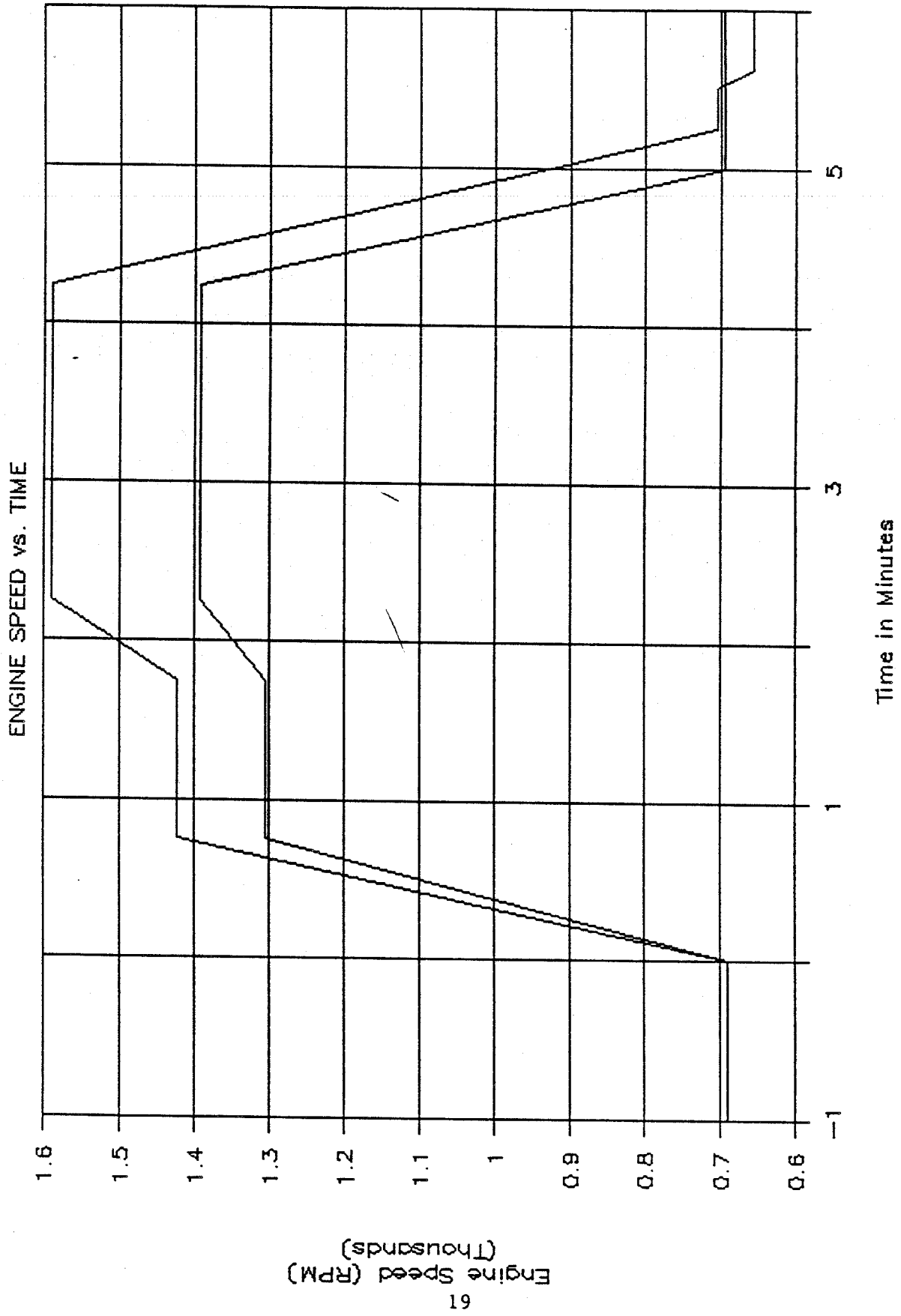
Figure 5. Graph of the heavy duty diesel truck cycle used to simulate a federal test procedure.

The first phase of the test allowed the vehicle operator to run through the cycle to become familiar with the sequence. The vehicle was then run through the cycle which was repeated until adequate filter loadings were achieved.

This simulated FTP for heavy duty trucks was followed by a steady state test similar to that used for the light duty vehicles.

Filters were changed only once during each test with gasoline fueled vehicles and heavy duty diesel vehicles. The filters loaded much more rapidly with the light duty diesel tests. In this case, filters were changed during the FTP. As a result, more than one set of filters represent this test cycle for the light duty vehicles. The single stage dilution sampler was used with the first two light duty diesel vehicles tested, and filters had to be changed at different stages of the FTP. The single stage sampler was then replaced with the two stage dilution sampler, after which filters were replaced only during the cold soak portion of the test between the cold stabilized phase II of the test and the hot transient phase III of the CVS-75 FTP illustrated below:

	I Cold		II Cold		Cold Soak		III Hot	
START	Transient 505 seconds		Stabilized 870 seconds		(Filters Changed) 600 seconds		Transient 505 seconds	STOP
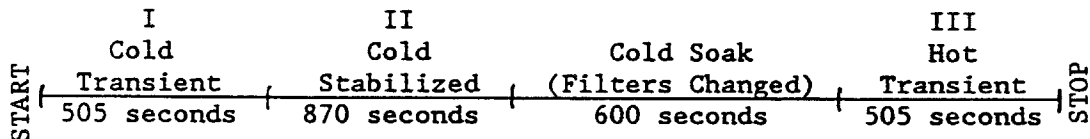
The sequence of vehicles tested started with catalyst equipped vehicles using unleaded gasoline, followed by light duty diesel, non-catalyst equipped vehicles using leaded gasoline, and heavy duty diesel vehicles. This sequence of sampling minimized any possible cross contamination between vehicle types even though the samplers were thoroughly cleaned before testing the next vehicle type. The dichotomous virtual impactors were completely disassembled and cleaned with soap and water, and then rinsed with ethanol between testing different fuel type groups. The entire dilution

20

chamber was cleaned with alcohol after the light duty diesel vehicles tests. It was cleaned again with a pressurized steam cleaner after testing the vehicles using leaded gasoline and before testing the heavy duty diesel trucks.

3.1.5 Filter Collimation

The 37 mm diameter coarse particle filters were collimated to a diameter of 0.6 cm to compensate for the much lower abundance of this size particle (2.5-10 μm) relative to fine (< 2.5 μm) particles in vehicle exhaust. This smaller deposit area provided more nearly equal analytical sensitivities for both fine and coarse particles, since the analytical methods used depended on the deposit per cm^2. This improved the elemental analysis sensitivity, but not the deposit mass determination which depends on mass per total filter.

3.2 Tunnel Sample Collection

3.2.1 Tunnel Characteristics

Sepulveda Tunnel and background aerosol samples were collected as part of this study to establish a source profile for on-road vehicle emissions and to estimate the uncertainty in composite airshed vehicle emissions established from tailpipe exhaust measurements. The Sepulveda Tunnel was selected for this study because, of the tunnels in the SCAB, it comes closest to meeting selection requirements which included availability of power, length greater than one quarter mile, level, etc. (20).

The tunnel and surrounding area are schematically illustrated in Figure 6. Sepulveda Boulevard is a north/south street that passes under the Los Angeles International Airport runway for a distance of 0.36 miles. There is a slight incline (2% slope) at both ends of the tunnel, and there are major intersections with a stop light one half mile to the north (Century Blvd.) and one quarter mile to the south (Imperial Highway). The immediate area around the tunnel is characterized as commercial or light industrial.

LAX AIRPORT RUNWAY

NORTHBOUND
SEPULVEDA BLVD.

TUNNEL ACCESS
BUILDING

VENT DUCT

TUNNEL
0.36 MILES

DIVIDER

EMERGENCY PULL OUT AREAS

VENT DUCT

LOCATION OF TUNNEL
SAMPLING STATION

LOCATION OF
AMBIENT SAMPLER

SOUTHBOUND
SEPULVEDA BLVD.
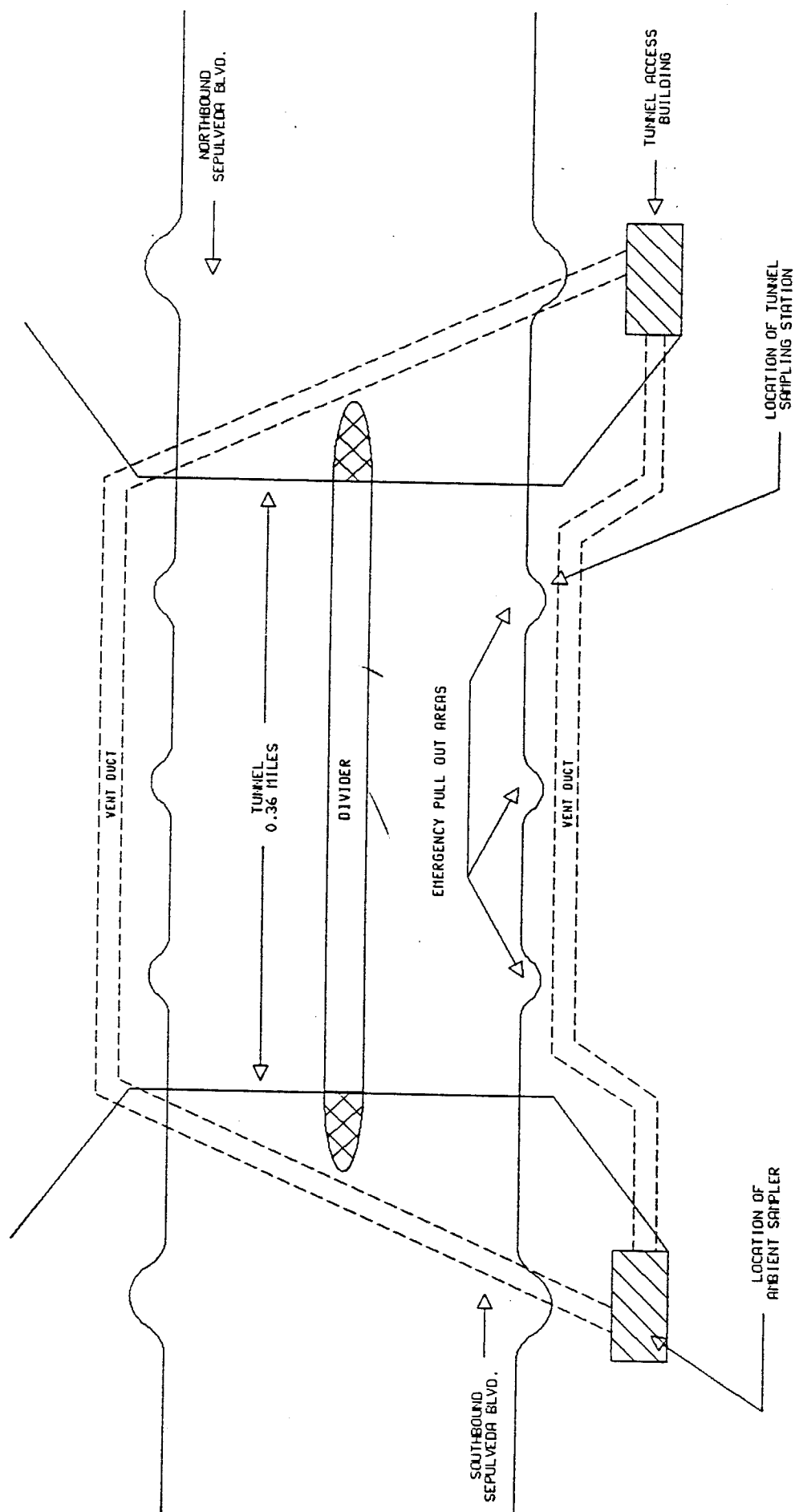
FIGURE 6.   Schematic illustration of the Sepulveda Tunnel
and surrounding area.

22

The other major characteristic features of the area are the airport, a large oil refinery about one mile to the southwest, and the Pacific Ocean about one mile to the west.

The tunnel contains six lanes for traffic, with two pullouts at either end of the tunnel. Ventilation ducts run on the sides of the tunnel parallel to the traffic, and fan buildings are located at each end of the tunnel. The natural ventilation in the tunnel is usually adequate and fans are rarely required. They were not in operation during any of our three sampling periods.

Natural ventilation draws tunnel air into the vent ducts through a series of slits in the wall separating the traffic lanes from the vent ducts. Outside air is forced into the tunnel by the ramming action of the vehicles entering the tunnel.

3.2.2 Samplers

The same sampling chamber used to collect exhaust particles was used to collect tunnel aerosol samples. The 4 inch diameter stainless steel inlet pipe was extended into a vent slot 100 feet from the south end of the tunnel on the west side (southbound traffic) at a height of about 8 feet above the roadway. Tunnel air was drawn into the dual sampling chambers at a rate of about 100 cfm, with a high volume blower located downstream of the sampling chamber. Fine and coarse particle samples were collected with Sierra Model 244 manual dichotomous samplers with a 10 μm inlet.

Samples for gas analysis were collected at the same point as the particle samples using a bag sampler provided by the SCAQMD ~~SCAB~~. The gas samples collected during the last two sampling periods were incomplete because the connecting hoses were disconnected at some unknown time into the sampling period.

Samples of the background aerosol were collected simultaneously with the tunnel samples, using similar sampling equipment located on top of the north ventilation fan building.

Tunnel samples were collected during three different peak traffic periods to provide maximum tunnel aerosol concentration to background ratios. The first sampling period was from 6:50 AM to 10:00 AM on Thursday morning, September 25, 1986, which was followed by a second sampling period in the afternoon from 2:40 PM to 6:30 PM. The third sampling period was on Sunday, September 28, 1986, from 11:00 AM to 3:00 PM.

3.2.3 Meteorology

Meteorological data was recorded at a ~~SCAQMD~~ National Weather Service station located a few hundred yards northwest of the background monitor. The temperature, relative humidity, wind direction, wind speed, and pressure are summarized for the sampling periods in Table 2.

It had rained steadily throughout the night preceding the Thursday morning sampling period, stopping only a few hours before the start of our first sampling period. The winds were consistently out of the west, ranging from calm for a brief period on Thursday morning to a high of 17.3 mph on Thursday afternoon. The relative humidity was highest right after the rain (93%) and declined to a low of 63% on Sunday afternoon.

3.2.4 Traffic Characteristics

The SCAQMD used video recordings of the southbound tunnel traffic to determine the characteristics of the vehicle distribution during each sampling period. The traffic was separated into light duty vehicles using gasoline and diesel fuels and heavy duty diesel vehicles. The gasoline fueled vehicles were further separated into catalyst and non-catalyst equipped vehicles based on

24

Table 2
METEOROLOGICAL DATA ON TUNNEL TEST DAYS

Date	Time (PDT)	Temp (°F)	RH (%)	Wind Dir. (degrees)	Wind Speed (mph)	Pressure (millibars)
Thursday 9/25/86	0600	59	90	240	10.4	1010.2
	0700	57	93	230	4.6	1010.6
	0800	61	84	Calm	Calm	1011.6
	0900	62	78	250	6.9	1012.2
	1000	63	75	250	9.2	1013.2
	1100	65	75	240	13.8	1013.6
	1200	66	70	230	15.0	1013.6
	1300	67	68	240	15.0	1013.4
	1400	68	68	230	15.0	1013.1
	1500	68	68	230	16.1	1013.0
	1600	68	68	240	17.3	1012.8
	1700	67	75	230	16.1	1012.7
	1800	65	78	240	16.1	1013.0
	1900	65	73	240	13.8	1013.2
Sunday 9/28/86	1100	66	68	260	6.9	1014.6
	1200	67	65	260	11.5	1014.2
	1300	67	63	260	11.5	1013.8
	1400	68	65	260	12.7	1013.4
	1500	68	65	260	12.7	1012.7

25

the model year of the vehicle. Vehicles newer ~~than 1975~~ were
assumed to be catalyst equipped, while older model year vehicles
were assumed to be non-catalyst equipped. This classification did
not define the number of ~~median~~ medium and heavy duty non-catalyst vehicles
using leaded gasoline.

The vehicle type distribution is summarized in Table 3.
The number of vehicles listed include only the southbound traffic
videotaped during our sampling periods. The vehicle distribution
was reasonably constant on all three days with 89.2 ± 0.5% of the
vehicles consisting of catalyst equipped light duty vehicles. Non-
catalyst equipped light duty vehicles comprised 6.3 ± 0.4% of the
vehicles. Diesel fueled vehicles accounted for the remaining
vehicles, with light duty diesel vehicles responsible for 2.1% of
the traffic and 1.5% due to heavy duty vehicles.

The traffic operating pattern in the tunnel was
perturbed from its normal pattern on Thursday because the tunnel
lighting had been reduced due to a power outage in the Airport. As
a result, the traffic slowed drivers applied their brakes and as it entered the tunnel ~~by applying their brakes~~. This braking, deceleration, and resumed acceleration
on exiting the tunnel represents a substantial deviation from the
normal steady state traffic pattern which had been anticipated.

3.3 Analytical Methods

3.3.1 Mass

Deposit mass was determined using a Cahn Electrobalance
Model 27. It was calibrated with class M standards traceable to NBS
standards. Ten percent of the filters were reweighed by an indepen-
dent technician. NEA's last independent audit for mass determina-
tion was September, 1986 (40).

Table 3

TUNNEL TRAFFIC COUNTS AND VEHICLE MILES TRAVELED[a]

Sampling Period	Total No. Vehicles[b]	LDV – Unleaded			LDV – Leaded			LDV – Diesel			HDV – Diesel		
		No.	%	VMT[c]	No.	%	VMT[c]	No.	%	VMT[c]	No.	%	VMT[c]
9/25/86 0650-1000	7388	6556	88.7	2386 (119)[d]	498	6.7	181 (9)	154	2.1	56 (3)	132	1.8	48 (2)
9/25/86 1440-1830	9976	8948	89.7	3257 (163)	628	6.3	229 (11)	210	2.1	76 (4)	120	1.2	44 (2)
9/28/86 1100-1500	6192	5516	89.1	2008 (100)	366	5.9	133 (7)	130	2.1	47 (2)	96	1.6	35 (2)

a. Based on one way southbound traffic

b. Includes motorcycles (9/25/86, 0650-1000, motorcycles = 48 (0.7%)

c. Number of vehicles multiplied by tunnel length (0.364 miles)

d. Uncertainties are listed in parentheses

Filter samples returned to the laboratory were equili-
brated for at least twenty-four hours at 50 ± 5% relative humidity
and 72 ± 5°F prior to weighing.

3.3.2 Elemental Analysis

Each Teflon filter was analyzed for Al, Si, P, S, Cl, K,
Ca, Ti, V, Cr, Mn, Fe, Ni, Cu, Zn, Ga, As, Se, Br, Rb, Sr, Y, Zr,
Mo, Pd, Ag, Cd, In, Sn, Sb, Ba, La, Ce, Hg, and Pb using an ORTEC
TEFA III energy dispersive X-ray fluorescence analyzer. The filters
were analyzed in vacuum in groups of ten filters, along with a blank
and quality control filter using three different excitation condi-
tions to optimize sensitivities for specific groups of elements as
indicated below:

Condition 1		Elements Measured
Anode:	Mo	Fe, Ni, Cu, Zn, Ga, As, Se, Br, Rb,
Filter:	Mo	Sr, Y, Zr, Mo, Pd, As, Cd, In, Sn,
Voltage:	50 KeV	Sb, Ba, La, Hg, and Pb

Condition 2		
Anode:	Mo	Na*, Mg*, Al, Si, P, Fe
Filter:	None	
Voltage:	15 KeV	*Not quantified

Condition 3		
Anode:	W	S, Cl, K, Ca, Ti, V, Cr, Mn, Fe, Br,
Filter:	Cu	Mo, Cd, Ba, La, Ce, Nd, Pb
Voltage:	35 KeV	

Corrections were made for spectral interferences, self absorption,
and particle size effects. An NBS standard reference material
standards (SRM No. 1832 and 1833) were analyzed periodically to
assure the quality of the analysis.

The analyzer was calibrated using standards that have been
validated through theoretical evaluations, multiple standards
comparisons, interlaboratory comparisons, intermethod comparisons,
and are traceable to NBS standards. The most recent interlaboratory
comparison was in the spring and summer of 1986, which involved a

comparison of the analysis of 800 filters that had previously been analyzed by the Davis, California campus of the University of California cyclotron group (41). Prior to this intercomparison, our method was audited by the EPA using NBS standards in January, 1986 (42). Details of our quality control and quality assurance program results for this analysis are presented in Appendix B.

3.3.3 Carbon Analysis

Organic, elemental, and carbonate forms of carbon were determined using a combustion flame ionization method which includes a correction for pyrolysis of organic carbon during the analysis. This is a method-defined analysis for which NBS standards are currently not available.

The measurement was made on a 1.5 cm^2 punch from a 37 mm diameter quartz fiber filter. These quartz filters were sampled simultaneously with the Teflon filters analyzed by XRF. The quartz fiber filter was first heated to 680°C in the presence of He to determine the organic carbon. This was followed by the introduction of oxygen and reheating to 770°C to burn off the elemental carbon. The analysis was completed by the injection of a known amount of carbon for calibration. The details of the analysis are provided in Volume III, Appendix C, of this report.

4.0 RESULTS AND DISCUSSION

4.1 Vehicle Exhaust

Individual vehicle testing results are summarized in Appendices C-N. Carbon analysis results are presented in Appendix C and the characteristics of the vehicles tested and filter identifications are listed in Appendix D. Appendices E-L summarize the individual vehicle chemical analysis results. Gaseous and particulate emission factors are summarized in Appendices M and N.

The average vehicle exhaust source profiles are provided in Volume II of this report as profiles 1-07 through 1-14. Two examples of the resulting profiles in tabular form are presented in Tables 4 and 5 and in histogram form in Figure 7. The average emission factors for both gases and particles are summarized by vehicle type in Table 6. Emission factors for the two diesel trucks sampled were not measured because of vehicle testing limitations.

The uncertainties listed for the source profiles are the standard error of the mean. Both the standard error and the standard deviation are listed for the emission factors in Table 6. The range of emission factors within a vehicle category was substantially greater for particles than for gases. The relative standard deviation for particulate emission factors is about 100%, while it is generally less than 50% for the gaseous species.

The emission rates for FTP emissions are substantially higher than for the SS emissions. The emission rates for the gases are generally 2-3 times greater during the FTP. The particle emission rates for the diesel and leaded gasoline fueled vehicles during the FTP are about ten fold greater than the SS testing procedure. The SS emission rate for catalyst equipped vehicles using unleaded gasoline, however, is only about a factor of two less than the FTP.

Although there was a high degree of emission rate variability between the two test procedures and vehicles within the same category, the relative composition of the major species showed less variability. For example, the average fine particle Pb concentration in the FTP LDV-L emissions was 21.6% and 18.0% in the SS emissions. In addition, the elemental carbon in the fine fraction LDV-D emissions were 66 and 63% for the FTP and SS tests respectively. Even the HDD elemental carbon (EC) wasn't greatly different at 52% for the simulated FTP.

Table 4

COMPOSITED VEHICLE EXHAUST PROFILE
Standard Error

srce code	part size	revsion date	source description		reference	date
5398	FCT	07/07/87	LEADED, steady state	SCAB	1	04/87

P E R C E N T C O M P O S I T I O N

SPECIES	FINE	COARSE	TOTAL
Al	.6697 +- 1.1463	.6927 +- 1.1716	.4915 +- .9530
Si	1.5878 +- .6408	.1986 +- .1909	1.3350 +- .5828
P	.4348 +- .1347	.0697 +- .1649	.3736 +- .1304
S	.0224 +- .9076	.0000 +- 1.4388	.0159 +- .7616
Cl	.0507 +- .1546	.0576 +- .2338	.0621 +- .1274
K	.1328 +- .0568	.0275 +- .0227	.1124 +- .0384
Ca	.1016 +- .0575	.1492 +- .1747	.1028 +- .0605
Ti	.0028 +- .0085	.0079 +- .0612	.0032 +- .0154
V	.0037 +- .0065	.0070 +- .0254	.0040 +- .0073
Cr	.0007 +- .0067	.0344 +- .0196	.0067 +- .0051
Mn	1.3450 +- .8783	.3031 +- .1892	1.1688 +- .8084
Fe	.0204 +- .0250	.0648 +- .0644	.0234 +- .0201
Ni	.0141 +- .0073	.0201 +- .0178	.0135 +- .0052
Cu	.0313 +- .0089	.0110 +- .0114	.0274 +- .0066
Zn	.1091 +- .0149	.0835 +- .0784	.0976 +- .0220
Ga	.0377 +- .0315	.0050 +- .0501	.0307 +- .0263
As	.1820 +- .5047	.0000 +- .8287	.1332 +- .4261
Se	.0000 +- .0079	.0045 +- .0088	.0014 +- .0060
Br	10.3652 +- 1.1864	1.4290 +- 1.1873	8.4454 +- 1.0998
Rb	.0000 +- .0677	.0000 +- .0875	.0000 +- .0551
Sr	.0000 +- .0131	.0000 +- .0096	.0000 +- .0096
Y	.0011 +- .0353	.0000 +- .0514	.0010 +- .0289
Zr	.0000 +- .0723	.0000 +- .0475	.0000 +- .0525
Mo	.0000 +- .0422	.0000 +- .0281	.0000 +- .0306
Pd	.0000 +- .0437	.0000 +- .0280	.0000 +- .0317
Ag	.0000 +- .0577	.0000 +- .0368	.0000 +- .0418
Cd	.0000 +- .0762	.0000 +- .0478	.0000 +- .0552
In	.0000 +- .0941	.0000 +- .0601	.0000 +- .0682
Sn	.0000 +- .1152	.0000 +- .0726	.0000 +- .0833
Sb	.0000 +- .2525	.0000 +- .1602	.0000 +- .1827
Ba	.0000 +- .4763	.0000 +- .3017	.0000 +- .3450
La	.0000 +- .8675	.0000 +- .5479	.0000 +- .6287
Hg	.0014 +- .0098	.0158 +- .0165	.0030 +- .0073
Pb	17.9917 +- 1.8857	3.7056 +- 2.9785	15.0562 +- 2.4468
OC	51.8472 +- 4.4239	13.7912 +-12.3626	48.9879 +- 4.8730
EC	1.3222 +- 1.0299	1.4286 +- 2.2589	1.2972 +- 1.2255
Sum	86.2754	22.1068	77.7939

Table 5

COMPOSITED VEHICLE EXHAUST PROFILE
Standard Error

srce code	part size	revsion date	source description		reference	date
5397	FCT	08/08/87	LEADED, federal test	SCAB	1	04/87

PERCENT COMPOSITION

SPECIES	FINE	COARSE	TOTAL
Al	.6415 +- .6415	.3422 +- .6991	.5992 +- .5773
Si	.7856 +- .4601	.2816 +- .2013	.7197 +- .3583
P	.1674 +- .1802	.1223 +- .1218	.1678 +- .1109
S	.0000 +- 1.2081	.0000 +- 2.1640	.0000 +- 1.0121
Cl	.2624 +- .2624	.0000 +- .3359	.2383 +- .2383
K	.0511 +- .0254	.0128 +- .0236	.0446 +- .0214
Ca	.0918 +- .0288	.2945 +- .1514	.1069 +- .0341
Ti	.0040 +- .0023	.0170 +- .0210	.0043 +- .0049
V	.0018 +- .0017	.0044 +- .0083	.0018 +- .0022
Cr	.0012 +- .0018	.0326 +- .0111	.0055 +- .0022
Mn	.9873 +- .6120	1.2045 +- .3039	.9559 +- .5337
Fe	.1113 +- .0451	.8489 +- .2298	.1975 +- .0513
Ni	.0120 +- .0046	.0255 +- .0074	.0134 +- .0051
Cu	.0264 +- .0056	.0385 +- .0084	.0278 +- .0056
Zn	.1483 +- .0395	.3921 +- .0852	.1809 +- .0406
Ga	.0311 +- .0414	.0053 +- .0746	.0244 +- .0344
As	.0093 +- .6977	.0000 +- 1.2619	.0089 +- .5809
Se	.0000 +- .0061	.0065 +- .0107	.0026 +- .0051
Br	6.1834 +- 2.1128	6.1473 +- 2.2119	6.0207 +- 2.1370
Rb	.0052 +- .0456	.0000 +- .0873	.0048 +- .0397
Sr	.0000 +- .0050	.0000 +- .0075	.0000 +- .0042
Y	.0000 +- .0412	.0000 +- .0832	.0000 +- .0345
Zr	.0000 +- .0219	.0000 +- .0280	.0000 +- .0181
Mo	.0000 +- .0108	.0000 +- .0096	.0000 +- .0088
Pd	.0000 +- .0115	.0000 +- .0225	.0000 +- .0123
Ag	.0000 +- .0146	.0000 +- .0137	.0000 +- .0121
Cd	.0000 +- .0200	.0000 +- .0464	.0000 +- .0236
In	.0000 +- .0242	.0000 +- .0216	.0000 +- .0199
Sn	.0000 +- .0293	.0000 +- .0397	.0000 +- .0268
Sb	.0000 +- .0639	.0000 +- .0554	.0000 +- .0523
Ba	.0000 +- .1195	.0000 +- .1030	.0000 +- .0977
La	.0000 +- .2203	.0000 +- .1902	.0000 +- .1802
Hg	.0015 +- .0048	.0136 +- .0084	.0031 +- .0040
Pb	21.6486 +- 7.6498	30.6310 +- 6.8840	23.1220 +- 8.1656
OC	31.3744 +-19.8383	3.7681 +- 3.3089	28.8997 +-19.9465
EC	15.0527 +- 2.4341	7.2203 +- 5.5383	12.7359 +- 4.5216
Sum	77.5983	51.4090	74.0857
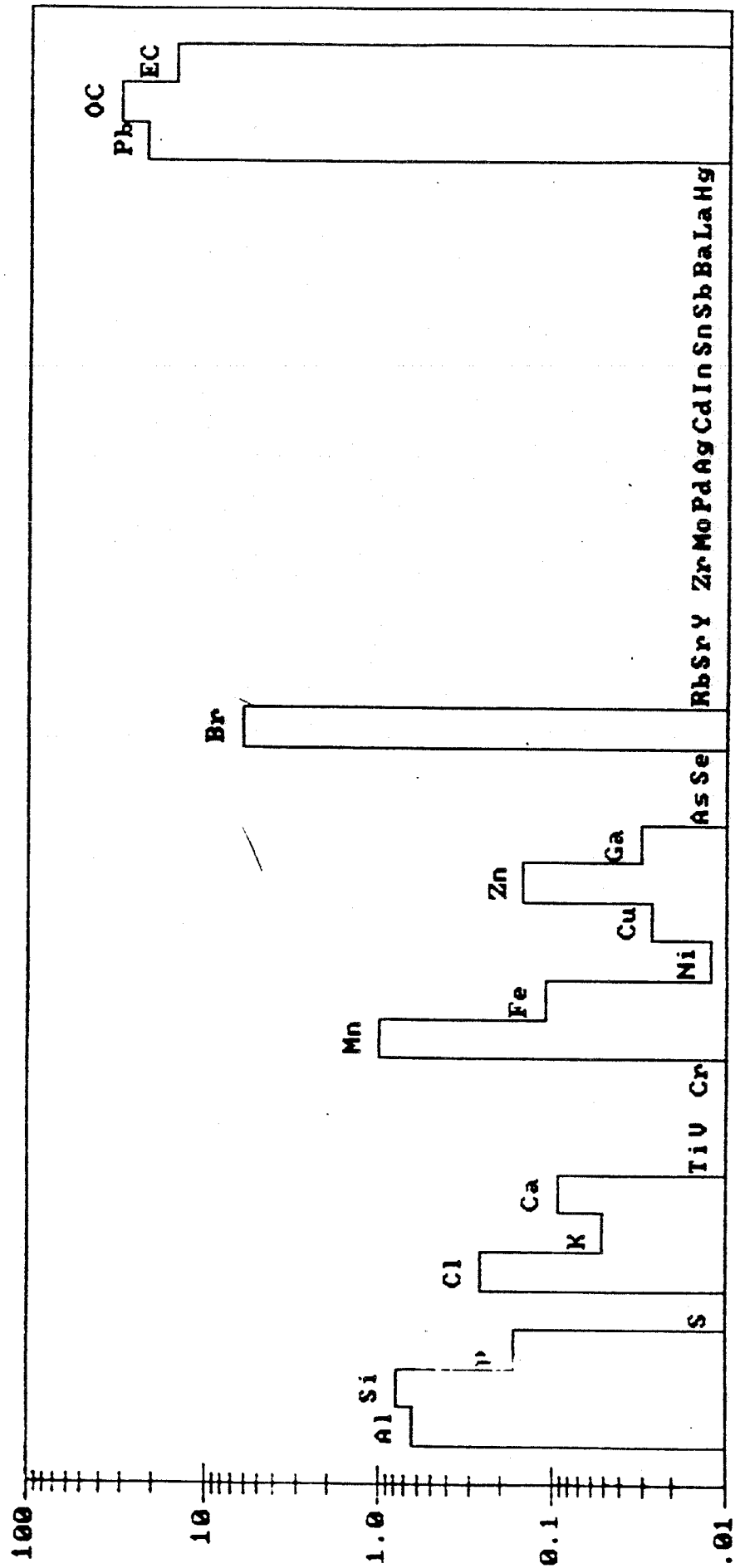
Figure 7. Histogram profile for tailpipe exhaust emissions from a light duty vehicle using leaded gasoline during a federal test procedure.

33

Table 6

AVERAGE TAILPIPE EMISSION FACTORS[a]

Vehicle Type	Test	Size	Particles (mg/mile)	Gases (g/mile)					
				HC	CH_4	CO	CO_2	NO	NO_4
LDV-U n=6	FTP	F	7.5 ± 4.9 (2.0)						
		C	1.8 ± 0.5 (0.2)						
		PM_{10}	9.3 ± 4.9 (2.0)	0.65 ± 0.27 (0.11)	0.14 ± 0.10 (0.04)	16.7 ± 18.5 (7.6)	805 ± 201 (82)	0.90 ± 0.46 (0.19)	1.6 ± 0.8 (0.3)
	SS	F	4.3 ± 7.8 (3.2)						
		C	0.7 ± 0.2 (0.1)						
		PM_{10}	5.1 ± 7.9 (3.2)	0.09 ± 0.04 (.02)	0.05 ± 0.03 (.01)	0.63 ±	467 ± 179 (73)	0.40 ± 0.33 (0.13)	0.71 ± 0.64 (0.26)
LDV-L n=4	FTP	F	98 ± 76 (38)						
		C	38 ± 64 (32)						
		PM_{10}	135 ± 135 (68)	7.8 ± 2.7 (1.4)	0.46 ± 0.31 (.15)	113 ± 55 (27)	473 ± 96 (48)	1.0 ± 0.9 (0.4)	2.3 ± 1.3 (0.6)
	SS	F	10.1 ± 5.0 (2.5)						
		C	2.3 ± 2.0 (1.0)						
		PM_{10}	12.4 ± 5.3 (2.6)	2.1 ± 0.8 (0.4)	<	50 ± 34 (17)	302 ± 71 (36)	0.43 ± 0.27 (0.14)	0.83 ± 0.65 (0.33)
LDV-D n=4	FTP	F	2190 ± 2150 (1080)						
		C	110 ± 60 (30)						
		PM_{10}	2300 ± 2210 (1100)	0.81 ± 0.46 (0.23)	<	4.1 ± 1.6 (0.8)	1200 ± 400 (200)	2.7 ± 1.0 (0.5)	5.6 ± 2.1 (1.0)
		F	298 ± 218 (109)						
		C	15 ± 8 (4)						
		PM_{10}	313 ± 225 (112)	0.20 ± 0.13 (0.06)	<	0.93 ± 0.48 (0.24)	347 ± 126 (63)	0.99 ± 0.48 (0.24)	2.0 ± 0.9 (0.4)

a. Uncertainties listed are standard deviations and standard errors are listed in parenthesis.

In contrast, the elemental carbon composition showed a high degree of variability between the two tests for the gasoline powered vehicles. The FTP to SS test EC composition ratio was 8.0 for fine particle emissions from LDV-U and 11.4 for LDV-L.

The concentration of Zn, which is thought to be primarily from motor oil, was the most constant of all species between all vehicle types. The average concentration for all vehicles was 0.14%, with a standard deviation of only 0.19%. The Zn concentration had much less variability within the diesel category (0.045 ± 0.006%) exhibiting a relative standard deviation of only 13%. Although the variability was almost 100% within the gasoline category, most of this variability was due to the unleaded FTP value of 0.59%. The mean and standard deviation of the other three categories was 0.124 ± 0.021%.

The variability in the concentration of the other elements was generally less for the SS tests than for the FTPs. For example, the standard deviations for Br, Pb, and organic carbon (OC) were between 3-10 fold less for the SS tests than in the FTP emissions.

The ratio of the mean fine particle Br and Pb concentrations for the LDV-L emissions was 0.29 for the FTP, and 0.58 during the SS tests. The mean coarse particle Br to Pb ratio was 0.20 and 0.39 for the tests.

The concentration of Mn in the LDV-L emissions was relatively high at about 1% in the fine particle emissions, presumably due to Mn additives to the gasoline.

The concentration of S was highest in the LDV-U emissions at about 5%, but was less than about 1% in the other emission categories.

The Si concentration was also highest in the LDV-U SS emissions. The mean SS fine particle concentration was 6.2%.

Several of the samples from the LDV-U emissions gave indications of trace levels of Ce. As a result, all of the filter samples from the unleaded gasoline vehicle tests were reanalyzed under conditions that provided improved detection limits for rare earth elements. Under these conditions, Ce was detected on two filters; one sample was of coarse particles from a FTP test of a 1980 Buick Regal, (Vehicle No. 5), and the other was of coarse particles from a 1982 Toyota Corona (Vehicle No. 4). The Ce concentration was 11.7 ± 1.2 ng/cm^2 in the Buick emissions and 98.3 ± 6.4 ng/cm^2 in the Toyota emissions. The Ce to Si ratios were 0.071 ± 0.009 and 0.086 ± 0.005 for the Buick and Toyota emissions, respectively. The Ce concentrations were a few tenths of a percent, but highly uncertain because of the high uncertainty in the deposit mass. The source of the Ce is thought to be the catalyst substrate.

4.2 Tunnel Aerosol Measurements

4.2.1 Particulate Mass Concentrations

Particulate mass loadings during the three tunnel sampling periods are summarized in Table 7. The highest tunnel PM_{10} concentration of 113.3 $\mu g/m^3$ was obtained on Thursday morning. The tunnel concentrations dropped during the next two sampling periods to the lowest concentration of 79.2 $\mu g/m^3$ on Sunday. The background concentration was highest during the second sampling period on Thursday afternoon. Although the background dropped from a high of 39.6 $\mu g/m^3$ on Thursday afternoon to its lowest concentration of 27.9 $\mu g/m^3$ on Sunday, the net difference between the tunnel and background was highest during the first sampling period.

Table 7

SUMMARY OF PARTICULATE MASS CONCENTRATIONS
DURING TUNNEL SAMPLING PERIODS

Period	Size	Tunnel	F/C Ratio	Background	F/C Ratio	Bkg/Tun. Ratio	Net	F/C Ratio
Thurs AM	F	72.6 ± 7.9	1.8	19.3 ± 3.7	1.3	0.27	53.3 ± 8.7	2.1
	C	40.7 ± 5.2		14.8 ± 3.5		0.36	25.9 ± 6.0	
	PM_{10}	113.3		34.1		0.30	79.2	
Thurs PM	F	61.4 ± 6.7	1.5	15.6 ± 3.0	0.65	0.25	45.8 ± 7.3	2.8
	C	40.2 ± 4.8		24.0 ± 3.5		0.60	16.2 ± 5.9	
	PM_{10}	101.6		39.6		0.39	62.0	
Sunday	F	51.0 ± 5.7	1.8	15.2 ± 2.9	1.2	0.30	35.8 ± 6.4	2.3
	C	28.2 ± 3.8		12.7 ± 2.8		0.45	15.5 ± 4.7	
	PM_{10}	79.2		27.9		0.35	51.3	
Mean	F	61.7 ± 10.8	1.7 ± 0.2	16.7 ± 2.3	1.0 ± 0.4	0.27	45.0 ± 8.8	2.4 ± 0.4
	C	36.4 ± 7.1		17.3 ± 6.0		0.47	19.2 ± 5.8	
	PM_{10}	98.0 ± 17.3		33.9 ± 5.9			64.2 ± 14.1	

About two thirds of the tunnel aerosol was associated with fine particles, while on the average, the background aerosol was about equally divided into fine and coarse particles. The net tunnel aerosol mass was 70% fine particles.

The characteristics of the tunnel aerosol were reasonably constant over the three sampling periods, while the background aerosol characteristics changed significantly. For example, although the average background fine to coarse particle ratio was 1.0, the ratio was only 0.65 on Thursday afternoon, but 1.3 and 1.2 on the other two sampling periods. In addition, the coarse particle concentration on Thursday afternoon was about twice the concentration on the other two sampling periods, while the fine particle concentration was equal to or slightly less. The coarse particle background to tunnel ratio was also much higher on Thursday afternoon than on the other two days.

4.2.2 Chemical Composition

The average chemical composition of the fine and coarse particle fractions in the tunnel and background particles during the three sampling periods are listed in Appendix O and summarized for selected species in Tables 8 and 9. The net tunnel aerosol concentrations are presented in Appendix P in $\mu g/m^3$ and percent of total deposit mass in each size fraction. Background to tunnel ratios, as well as fine to coarse particle ratios, are also presented in this Appendix for each species along with ratios to Pb and Si. The net tunnel particulate concentrations and background to tunnel ratios for selected species are listed in Tables 10 and 11.

Organic and elemental carbon are the most abundant species in the tunnel fine particle size fraction, while organic carbon is the most abundant species in the background fine particle size fraction. The concentration of most species were reasonably constant in the tunnel over the three sampling periods. A higher

38

Table 8

CONCENTRATION OF SELECTED CHEMICAL SPECIES
IN THE FINE AND COARSE PARTICLE SIZE FRACTIONS DURING THE SAMPLING PERIODS
($\mu g/m^3$)

Element	Size	Tunnel			Background		
		Thurs. AM	Thurs. PM	Sunday	Thurs. AM	Thurs. PM	Sunday
Si	Fine	0.732 ± 0.084	0.690 ± 0.079	0.443 ± 0.051	0.078 ± 0.015	0.067 ± 0.012	0.092 ± 0.014
S		1.289 ± 0.200	1.286 ± 0.195	1.138 ± 0.161	0.883 ± 0.108	0.863 ± 0.104	0.890 ± 0.106
Cl		0.695 ± 0.866	2.622 ± 0.297	0.117 ± 0.026	0.385 ± 0.048	2.513 ± 0.284	0.022 ± 0.012
Ca		0.169 ± 0.020	0.201 ± 0.024	0.113 ± 0.014	0.016 ± 0.005	0.072 ± 0.009	0.023 ± 0.005
Fe		1.252 ± 0.140	1.139 ± 0.128	0.750 ± 0.084	0.024 ± 0.005	0.005 ± 0.003	0.008 ± 0.003
Cu		0.060 ± 0.007	0.066 ± 0.008	0.037 ± 0.004	0.004 ± 0.002	0.007 ± 0.002	0.002 ± 0.001
Zn		0.132 ± 0.015	0.116 ± 0.013	0.096 ± 0.011	0.007 ± 0.002	0.000 ± -0.001	0.005 ± 0.001
Br		0.825 ± 0.092	0.268 ± 0.070	0.378 ± 0.042	0.022 ± 0.003	0.012 ± 0.002	0.010 ± 0.002
Pb		1.214 ± 0.136	1.206 ± 0.135	0.852 ± 0.096	0.072 ± 0.010	0.018 ± 0.005	0.036 ± 0.006
OC		25.06 ± 3.11	22.34 ± 2.74	17.24 ± 2.19	5.28 ± 1.30	2.75 ± 0.97	5.64 ± 1.13
EC		23.79 ± 2.79	19.09 ± 2.24	12.49 ± 1.55	3.31 ± 0.81	1.11 ± 0.58	1.17 ± 0.56
Si	Coarse	5.048 ± 0.567	4.772 ± 0.536	2.339 ± 0.264	0.442 ± 0.052	0.538 ± 0.062	0.875 ± 0.099
S		0.545 ± 0.094	0.671 ± 0.108	0.281 ± 0.071	0.457 ± 0.064	0.642 ± 0.083	0.170 ± 0.035
Cl		2.034 ± 0.232	4.839 ± 0.550	0.517 ± 0.062	3.036 ± 0.344	6.593 ± 0.746	0.697 ± 0.081
Ca		0.824 ± 0.094	0.879 ± 0.100	0.494 ± 0.056	0.132 ± 0.016	0.201 ± 0.024	0.125 ± 0.015
Fe		3.084 ± 0.348	2.908 ± 0.328	1.763 ± 0.199	0.158 ± 0.018	0.125 ± 0.014	0.188 ± 0.021
Cu		0.116 ± 0.013	0.120 ± 0.014	0.069 ± 0.008	0.036 ± 0.004	0.055 ± 0.006	0.048 ± 0.006
Zn		0.160 ± 0.018	0.142 ± 0.016	0.101 ± 0.012	0.008 ± 0.002	0.005 ± 0.001	0.009 ± 0.001
Br		0.049 ± 0.009	0.065 ± 0.010	0.044 ± 0.006	0.010 ± 0.002	0.006 ± 0.001	0.004 ± 0.001
Pb		0.380 ± 0.046	0.413 ± 0.050	0.419 ± 0.049	0.032 ± 0.006	0.011 ± 0.004	0.028 ± 0.005
OC		8.60 ± 1.55	8.69 ± 1.42	8.07 ± 1.35	0.35 ± 1.04	1.65 ± 0.93	0.06 ± 0.81
EC		2.02 ± 0.58	2.15 ± 0.53	2.14 ± 0.57	0.00 ± 0.64	0.00 ± 0.53	0.08 ± 0.51

Table 9

CONCENTRATION OF SELECTED CHEMICAL SPECIES
IN THE FINE AND COARSE PARTICLE SIZE FRACTIONS
DURING THE SAMPLING PERIODS

(Percent)

Element	Size	Tunnel			Background		
		Thurs. AM	Thurs. PM	Sunday	Thurs. AM	Thurs. PM	Sunday
Si	Fine	1.01	1.12	0.87	0.40	0.43	0.61
S		1.77	2.10	2.23	4.57	5.52	5.85
Cl		0.96	4.27	0.23	2.00	16.08	0.14
Ca		0.23	0.33	0.22	0.08	0.46	0.15
Fe		1.72	1.86	1.47	0.13	0.03	0.05
Cu		0.08	0.11	0.07	0.02	0.05	0.01
Zn		0.18	0.19	0.19	0.04	0.00	0.03
Br		1.14	1.02	0.74	0.11	0.08	0.07
Pb		1.67	1.97	1.67	0.37	0.11	0.23
OC		34.5	36.32	33.71	27.41	17.60	37.03
EC		32.7	31.04	24.42	17.19	7.09	7.69
Si	Coarse	12.4	11.80	8.31	2.98	2.24	6.91
S		1.34	1.67	1.00	3.09	2.68	1.35
Cl		4.99	1.00	1.84	20.50	27.50	5.50
Ca		2.02	2.18	1.76	0.89	0.84	0.99
Fe		7.57	7.22	6.26	1.07	0.52	1.48
Cu		0.28	0.30	0.24	0.24	0.23	0.38
Zn		0.39	0.35	0.36	0.06	0.02	0.07
Br		0.12	0.16	0.16	0.02	0.03	0.04
Pb		0.93	1.03	1.49	0.22	0.05	0.22
OC		21.1	21.65	28.78	2.34	6.89	0.49
EC		4.96	5.36	7.64	0.00	0.00	0.63

40

Table 10

NET TUNNEL SUSPENDED PARTICULATE CHEMICAL CONCENTRATIONS
(Percent)

Element	Size	Thurs. AM	Sampling Period Thurs. PM	Sunday
Si	Fine	1.23 ± 0.256	1.36 ± 0.28	0.98 ± 0.23
S		0.76 ± 0.444	0.92 ± 0.50	0.69 ± 0.55
Cl		0.58 ± 0.209	0.24 ± 0.90	0.26 ± 0.09
Ca		0.29 ± 0.061	0.28 ± 0.07	0.25 ± 0.06
Fe		2.30 ± 0.459	2.48 ± 0.48	2.07 ± 0.44
Cu		0.10 ± 0.022	0.13 ± 0.03	0.10 ± 0.02
Zn		0.23 ± 0.047	0.25 ± 0.05	0.25 ± 0.06
Br		1.51 ± 0.301	1.35 ± 0.26	1.03 ± 0.22
Pb		2.14 ± 0.433	2.60 ± 0.51	2.28 ± 0.49
OC		37.1 ± 8.76	42.8 ± 9.31	32.40 ± 9.00
EC		38.4 ± 8.31	39.3 ± 8.04	31.62 ± 7.29
Si	Coarse	17.8 ± 4.670	26.1 ± 10.0	9.45 ± 3.40
S		0.34 ± 0.446	0.18 ± 0.84	0.71 ± 0.56
Cl		-3.87 ± 1.84	-10.8 ± 7.0	-1.16 ± 0.75
Ca		2.67 ± 0.72	4.18 ± 1.66	2.38 ± 0.82
Fe		11.3 ± 2.94	17.2 ± 6.6	10.16 ± 3.35
Cu		0.31 ± 0.09	0.40 ± 0.18	0.13 ± 0.07
Zn		0.58 ± 0.15	0.85 ± 0.33	0.59 ± 0.20
Br		0.15 ± 0.05	0.36 ± 0.15	0.26 ± 0.09
Pb		1.34 ± 0.34	2.48 ± 0.96	2.52 ± 0.83
OC		31.8 ± 10.31	43.5 ± 19.1	51.68 ± 18.73
EC		7.8 ± 3.79	13.3 ± 6.7	13.29 ± 6.38

Table 11

BACKGROUND TO TUNNEL RATIOS FOR SELECTED SPECIES

Element	Size	Thurs. AM	Thurs. PM	Sunday
			Sampling Period	
Si	Fine	0.11 ± 0.02	0.10 ± 0.02	0.21 ± 0.04
S		0.68 ± 0.14	0.67 ± 0.13	0.78 ± 0.14
Cl		0.55 ± 0.10	0.96 ± 0.15	0.19 ± 0.11
Ca		0.10 ± 0.03	0.36 ± 0.06	0.20 ± 0.05
Fe		0.019 ± 0.004	0.004 ± 0.003	0.010 ± 0.005
Br		0.037 ± 0.005	0.02 ± 0.004	0.03 ± 0.006
Pb		0.06 ± 0.01	0.02 ± 0.004	0.04 ± 0.01
OC		0.21 ± 0.06	0.12 ± 0.05	0.33 ± 0.08
EC		0.14 ± 0.04	0.06 ± 0.03	0.09 ± 0.05
Na	Coarse	1.43 ± 0.07	1.36 ± 0.07	1.10 ± 0.08
Si		0.09 ± 0.01	0.11 ± 0.02	0.37 ± 0.06
S		0.84 ± 0.19	0.96 ± 0.20	0.61 ± 0.20
Cl		1.49 ± 0.24	1.36 ± 0.22	1.35 ± 0.22
Ca		0.16 ± 0.03	0.23 ± 0.04	0.25 ± 0.04
Fe		0.05 ± 0.008	0.04 ± 0.01	0.11 ± 0.02
Br		0.20 ± 0.05	0.10 ± 0.02	0.10 ± 0.03
Pb		0.08 ± 0.02	0.03 ± 0.01	0.07 ± 0.01
OC		0.04 ± 0.12	0.19 ± 0.11	0.01 ± 0.10
EC		0.00 ± 0.32	0.00 ± 0.25	0.04 ± 0.24

degree of variability was observed in the background aerosol. The Cl concentration showed the highest degree of variability. Its concentration was highest at 2.5 and 6.6 $\mu g/m^3$ in the fine and coarse particle fractions on Thursday afternoon in which Cl represented 16 and 28% of the deposit mass. The fine particle Cl concentration was one hundred fold lower on Sunday, and the coarse particle Cl concentration was down by ten fold.

The percent mass explained in the coarse particle size fraction is close to 100% if the metals are assumed to be in their oxide form, and a multiplying factor of 1.2 is applied to the organic carbon to account for H and O in the carbonaceous species. A smaller portion of the fine particle tunnel suspended particle mass is explained, but unmeasured species such as nitrate, ammonia, Na, Mg, and water could easily account for the unexplained mass. A significant portion of the background aerosol mass is not explained even when the above adjustments are taken into account. This is thought to be, in part, due to the large sea salt contribution and absorbed water. In addition, if the sulfur is present as Na_2SO_4, it will likely form its natural mineral, glaubers salt, which has ten waters of hydration; i.e., $NA_2SO_4 \cdot 10H_2O$.

The net tunnel fine and coarse particle concentrations are listed in Table 10. The most notable feature of this table is the net negative Cl concentration in the coarse particle size fraction, which is substantially greater than its uncertainty. This is also apparent in the background to tunnel ratios shown in Table 11. Here, the average background to tunnel Cl ratio in the coarse particle size fraction is 1.40 ± 0.08. In addition, the average percent relative uncertainty in this ratio is only 16%.

This finding for Cl suggests our original hypothesis that the aerosol in the tunnel is the sum of the background aerosol,

plus the aerosol generated by vehicles in the tunnel is incorrect, at least for some species. This finding suggests that

$$M_i^t = M_i^b + M_i^v - M_i^r$$

where

M_i^t = net total mass of species i in the tunnel

M_i^b = mass of ith species in the background aerosol

M_i^v = mass of ith species in the tunnel due to vehicles

M_i^r = mass of ith species removed in the tunnel

Loss of material under similar conditions has been previously reported. For example, Pierson and co-workers showed that about 15% of the mass of SO_2 and $SO_4^=$ emitted in tunnels was deposited either on the walls or in the gutter. Most of this sulfur loss, however, was due to SO_2 rather than removal of the $SO_4^=$ species (28,30).

The Cl removed in this particular case is in coarse particles and could be removed by impaction on vehicles or tunnel surfaces, or possibly removed chemically from the particulate phase through acid base type reactions. To provide further insight into this issue, each filter was analyzed again to determine the relative background to tunnel ratio for Na and to analyze under conditions that are optimum for measuring Ce, since Ce had been measured in the exhaust of two vehicles tested. Although no Ce was detected on any of the tunnel filter samples, background to tunnel Na ratios were determined and are listed for coarse particles in Table 11. Although the Na determination by XRF is not considered quantitative because of large matrix effects, the background to tunnel ratio should be relatively accurate because the matrix effects are expected to cancel in the ratio. The average Na background to tunnel ratio of 1.30 ± 0.17 was essentially the same, within the

experimental error, as the 1.40 ± 0.08 measured for Cl. The ratio
of the other species is less than 1.0. The only other coarse
particle species that is close to 1.0 is S, which is the fourth most
abundant species in sea water.

This suggests that the background to tunnel coarse
particle Cl and Na ratios of about 1.4 are due to the loss of the
marine aerosol through impaction. The following summary of observa-
tions are supportive of this hypothesis:

- The background to tunnel ratios for Na and Cl are 1.3
  and 1.4, respectively, while the ratios for the other
  elements are less than 1.0.

- The highest Cl concentrations were measured on Thursday
  afternoon when the wind speed was highest.

- The relative humidity at the background site on Thursday
  was in excess of 70% and probably substantially higher
  in the tunnel. At these relative humidities, it is
  likely that the marine particles are in the form of
  brine droplets (43).

- These high Cl concentrations followed a rain storm that
  lasted until just before our Thursday morning sampling
  started.

Based on this information, it is assumed for the rest of
this discussion that the loss of coarse particle Cl is associated
with a loss mechanism that affects only the marine aerosol and has a
relatively insignificant effect on the other species, except perhaps
the coarse particle S concentration. This removal means that the Cl
and possibly the S profile concentrations resulting from the tunnel
measurements are invalid.

Another interesting feature of the tunnel aerosol
chemistry is the fine particle Br to Pb ratio. This ratio ranged
from 0.45 to 0.70 with a mean of 0.55 ± 0.13, which is quite close
to the average value of 0.57 ± 0.11 measured in the LDV-L exhaust.

This ratio is substantially greater than the assumed stoichiometric ratio of 0.39, however, similar ratios have been reported for the Caldecott Tunnel in Oakland (23).

The concentration of the three gases measured in the tunnel and background are listed in Table 12. The total hydrocarbon THC and CO concentrations were quite variable over the three sampling periods. The difference in the CO levels are much larger, but the net concentration is highly variable. Of the three gas samples collected, the first is considered the most reliable because it is known to represent the entire sampling period.

4.3 Brake and Tire Wear Profiles

4.3.1 Overview

At the beginning of this project, the brake and tire wear contributions to PM_{10} particulate levels were thought to be small relative to tailpipe emissions based on previous studies. Pierson, et al (44,45), and Cadle (46), for example, concluded that tire wear contributions to the aerosol in tunnels and along freeways was about 1%. In addition, previous studies of brake wear had estimated emissions rates of a few mg per mile, substantially less than the tailpipe emissions factors in the mid-70's when these measurements were made.

Since these measurements were made, however, the average tailpipe emissions rates have decreased substantially, the number of vehicles have increased in many airsheds, the old asbestos brakes are being replaced, and new brakes have been introduced. Thus, the importance of tire and brake wear relative to vehicle tailpipe exhaust should have increased in the past decade since these previous studies.

Table 12

CONCENTRATION OF GASEOUS SPECIES
IN TUNNEL AND BACKGROUND (ppm)*

Date	Time (PDT)	Location	Bag ID	THC	CO_2	CO
9/25/86	0650-1000	Tunnel	571	3.5	373.6	5.6
		Background	534	2.9	333.9	2.6
		Net	–	0.6	39.7	3.0
9/25/86	1440-1830	Tunnel	578	4.5	447.8	19.5
		Background	507	3.1	336.5	0.9
		Net	–	1.4	111.3	18.6
9/28/86	1100-1500	Tunnel	537	4.1	404.1	6.8
		Background	627	3.3	321.7	0.6
		Net	–	0.8	82.4	6.2
	Mean Net Concentrations			0.93	77.8	9.27
	Standard Deviation			0.42	36.0	8.24

*By volume.

In addition, the results of this study indicate that a new "semi-metal" type of brake made substantial contributions to the tunnel particulate concentrations.

Although, we had not originally planned to characterize emission from these sources, additional effort was conducted in this area to review the literature and make selected quantitative and semiquantitative measurements of the profiles from these two source categories.

4.3.2 Tire Wear

The available information on tire wear emissions has limited relevance to PM_{10} particulate emissions from current tires. Most of the studies were conducted in the mid-1970's in tunnels, along freeways, or in laboratories (44-49). All of the reports concluded that most of the tire wear material was not airborne but there was substantial disagreement as to the aerosolizable tire wear fraction and its size distribution.

Pierson and Brachaczek (44,45) have reported airborne tire wear emission rates from their tunnel studies that ranged from 4 to 9 mg per tire mile, representing from 2 to 7% of the tire wear. In their study, airborne particles were defined by the sampler cut points which were about 20 μm. Special particle size distribution studies indicated a bimodal particle size distribution for particles with aerodynamic diameters less than 10 μm. About half of the PM_{10} mass was associated with particles having diameters in the range from 1 to 3 μm. The small particle mode was presumed to be due to devulcanization, while the large mode was assumed to be the fine particle "tail" of the normal mechanical wear distribution.

Similar results were found by Cadle and Williams (46). They found that less than 5% of tire wear was airborne, measured emissions rates of 1.6 mg per tire mile, and between 24% and 60% of

48

the emissions less than 10 μm had diameters less than 0.43 μm. These results are also in agreement with the results of Cardina (47) who found about 60% of the particles less than about 10 μm were greater than about 2.5 μm and about 40% less than 2.5 μm.

The above investigators characterized the rubber components of tire wear debris, but provided very little data on the elemental composition of tire wear emissions. The most extensive characterization of trace metal content of tires was done by Ondov (35). The average elemental content of his analysis of eleven tire samples is listed in Table 13 along with the organic and elemental content reported by Cass (2).

A semiquantitative determination of the elemental composition of tire rubber was made as part of this study. In general, the estimated concentrations were similar to those reported in Table 13 with a Zn concentration of 0.9%. Chlorine, which was estimated in this work at 1.5 ± 0.5% is substantially higher than the average concentration of 0.07 ± 0.006% reported by Ondov and suggests that there may have been some composition changes in the past fifteen years.

The profile listed in Table 13 is listed in the source library profile number 1-15. This profile is expected to be representative of the coarse particle fraction of tire wear emissions in the early 1970's, but may not be representative of coarse tire wear particles in 1986. The composition of the bulk tire material may also not be representative of the fine particle fraction because of potential differences in the mechanism with which these particles are formed.

Although the tire wear emission rate is not required for the source profile, it is required to develop a composite motor vehicle emission profile. The values reported by Pierson and Brachaczek (44,45) amd Cadle and Williams (46) are similar and

Table 13

COMPOSITION OF TIRES
(Percent)

Element	Composition (%)
Na	0.0537 ± 0.0125
Mg	0.0394 ± 0.0077
Al	0.0743 ± 0.0220
S	1.9889 ± 0.6935
Cl	1.5 ± 0.5*
Ca	0.0239 ± 0.0083
Ti	0.0164 ± 0.0048
V	0.0004 ± 0.0002
Mn	0.0003 ± 0.0001
Cu	0.0004 ± 0.0001
Zn	1.0182 ± 0.0469
Br	0.0005 ± 0.0001
Ba	0.0020 ± 0.0017
La	0.0003 ± 0.0001

*Estimated this work

suggest an emission rate of about 5 ± 3 mg per tire mile. These results, however, are for tunnel, freeway, or laboratory conditions and are not necessarily representative of emissions during typical driving conditions in the SCAB. The EPA suggests the use of 2 mg/mile in Appendix L of AP42, Volume II (49) based on the same references, but appears to us to be low. Pierson and Brachaczek (44,45) estimated that the average wear rate in the United States in the early 1970's was 150 mg per tire mile. Both Pierson and Brachaczek (44,45) and Cadle and Williams (46) found that about 5% of tire wear emissions are airborne, which suggests an emission rate of about 8 mg per tire mile for typical driving conditions. This tire wear emission rate is used in this study to represent typical driving in the SCAB. This emission rate, however, has a high degree of uncertainty because of the limited number of direct measurements.

4.3.3 Brake Wear

Very few studies of the chemical composition of brake wear emissions have been conducted. Two recent reports provide estimates of emission rates from asbestos brake pads, but provide no direct information on the chemical composition of their emissions. Muhlbaier and Williams (50), using a brake dynamometer, measured an airborne particulate emission rate of 10.8 mg/car mile. Cha, et al (53), measured an airborne emission rate of 3.8 mg/disc-brake mile or 12.8 mg/car mile, assuming front disk brakes and rear drum brakes. Cha, et al, also reported particle size data indicating 45% of the PM_{10} emissions were less than 2.5 μm diameter and 55% were between 2.5 and 10 μm (51).

Ondov reported the average concentration of about thirty elements in asbestos type brakes, as measured by neutron activation analysis. Concentrations for selected elements are listed in Table 14 and were used in the SCAB profile 1-17 reported in Volume II.

Table 14

COMPOSITION OF ASBESTOS BRAKE PADS
(Percent)

Element	Composition (%)
Na	0.0320 ± 0.0080
Mg	13.8000 ± 0.2000
Al	0.2150 ± 0.0550
Si	10.8 ± 1.0*
Cl	0.1450 ± 0.0150
Ca	1.8950 ± 1.7050
Sc	0.0006 ± 0.0002
V	0.0008 ± 0.0001
Cr	0.0977 ± 0.0222
Mn	0.0425 ± 0.0025
Fe	4.0000 ± 1.0951
Co	0.0068 ± 0.0016
Zn	0.3103 ± 0.0743
As	0.0013 ± 0.0001
Se	0.0000 ± 0.0000
Br	0.0000 ± 0.0002
Sr	0.0410 ± 0.0040
Sb	0.0002 ± 0.0001
Ba	0.9216 ± 0.4737
La	0.0001 ± 0.0000
Ce	0.0008 ± 0.0002

*Reference 22

52

As already noted, the results of the tunnel study conducted as part of this study lead to the identification of semi-metal brake pads as a new, significant source of metallic emissions from motor vehicles. No previous reports on either the emission rates or composition of emissions were found from our review of the literature.

A limited investigation into semi-metal brake pad emissions was conducted as part of this study because of the absence of literature values and the necessity to develop a source profile for this source to properly interpret the tunnel aerosol chemistry.

The chemical composition of semi-metal brake pad wear emissions were determined by collecting a sample of the emissions that had deposited on the wheel of a 1986 Acura. The deposit was transferred from the wheel to a small spot in the center of a pre-weighed 47 mm diameter ring mounted Teflon membrane filter and the deposit mass determined gravimetrically. The elemental composition was then determined by XRF analysis.

The results of this analysis are reported in Table 15. The validity of this profile is supported in part by the consistency of the tunnel data. First, the Cu to Fe ratio was calculated from the tunnel results after subtracting the estimated contribution made by other sources to these species. In the fine particle fraction, other sources contributed only about 10% of the Cu and Fe mass. The average excess Cu to Fe ratio in the three tunnel tests was 0.050 ± 0.004, in excellent agreement with the 0.049 ratio measured in the source profile. Secondly, the fine and coarse particle brake contributions obtained using this profile with CMB calculations on the tunnel aerosol data indicated that 43% of the brake wear was fine particles which is also in excellent agreement with the 45% obtained for asbestos brake wear by Cha, et al (51).

Table 15

EMISSION SOURCE PROFILE
FOR SEMI-METAL DISK BRAKE PADS (Percent)
(Acura, Semi-metal)

Element	Measured	Adjusted*
Fe	42.7 ± 3.6%	45.9 ± 3.9
Cu	2.10 ± 0.17	2.26 ± 0.18
Sn	0.60 ± 0.05	0.66 ± 0.05
Ba	3.21 ± 0.18	3.45 ± 0.19
Mo	0.34 ± 0.05	0.37 ± 0.05

*Adjusted for presence of road dust in sample

To obtain an indication of how representative this one source profile was of all semi-metal brake wear emissions, two new and two used brake pads were obtained and their elemental concentrations determined semiquantitatively. The results of these analyses are listed in Table 16. As noted, several additional species were measured in these pads. The most abundant species in all the pads was Fe. Barium was also present in all the pads at about the same relative composition as measured in the brake dust. Also measured in all the pads were Mg, Si, and Mn, but at much lower concentrations. Copper was observed only in the new brake pads that would be used to replace the Acura pads. Nickel and Zn were not observed in the new pads.

The elemental concentrations listed in Table 15 are reported for this source profile library in Volume II of this report. It should be noted, however, that this profile should be modified to include other species weighted by their estimated relative emissions.

4.4   Tunnel Composite Vehicle Emissions Profile

    4.4.1   Overview

A composite vehicle source profile was developed from the net tunnel suspended particulate composition by subtracting the contribution of road dust as indicated in Figure 1. The best estimate of the road dust contribution was established by CMB analysis of the net tunnel aerosol composition data set. The results of these CMB analyses are presented in Appendix Q and summarized in Table 17.

Although the primary function of this analysis was to provide the best estimate of the road dust contributions, the contributions other sources made and the quality of the fits can be used to evaluate the quality of the vehicle emissions profiles used in the CMB analysis.

Table 16

QUALITATIVE COMPARISON OF BRAKE PAD COMPOSITION

Element	PAD DESCRIPTION			
	New Honda[a]	New NAPA[b]	Used Small[c]	Used Large[c]
Mg	Minor	Minor	Minor	Minor
Al	-	-	-	Trace
Si	Minor	Minor	Minor	Minor
Cl	-	-	-	Trace
Ca	-	-	-	Trace
Mn	Trace	Trace	Trace	Trace
Fe	Major	Major	Major	Major
Ni	-	-	Trace	Minor
Cu	Major	-	-	-
Zn	-	-	Minor	Minor
Sr	Trace	-	Minor	Trace
Mo	Minor	-	-	-
Sn	Major	-	-	-
Ba	Major	Major	Major	Major

a. Part number 45022-SD4-A10, semi-metallic
b. Rayloc American Brakeblock, semi-metallic
c. Used semi-metal brake pads, brand and type unknown

Table 17

SOURCE CONTRIBUTIONS TO NET TUNNEL SUSPENDED PARTICULATE MASS

Source Category	μg/m³			Percent		
	Thurs. AM	Thurs. PM	Sunday	Thurs. AM	Thurs. PM	Sunday
FINE						
LDV-U-SS	ND	ND	ND	ND	ND	ND
LDV-L-SS	6.9 ± 1.1	6.4 ± 1.0	4.0 ± 0.6	13.0 ± 2.9	13.9 ± 3.1	11.1 ± 2.6
LDV-D-SS	26.2 ± 5.5	24.8 ± 4.8	13.8 ± 3.4	49.2 ± 13.1	54.1 ± 13.6	38.6 ± 11.6
Tire	10.2 ± 2.0	9.2 ± 1.8	7.6 ± 1.4	19.1 ± 4.8	20.0 ± 5.0	21.4 ± 5.4
Brake-Abs.	1.8 ± 1.8	1.4 ± 1.7	0.3 ± 1.2	3.4 ± 3.5	3.0 ± 3.7	0.7 ± 3.3
Brake-SM	2.4 ± 0.3	2.3 ± 0.3	1.5 ± 0.2	4.5 ± 0.9	5.1 ± 1.0	4.1 ± 0.9
T. Road Dust	2.2 ± 0.9	2.2 ± 0.9	1.8 ± 0.7	4.1 ± 1.9	4.8 ± 2.0	5.0 ± 2.0
Total	49.7 ± 6.3	46.3 ± 5.6	29.0 ± 3.9	93.3 ± 19.3	101 ± 20	80.9 ± 18.1
Measured	53.3 ± 8.7	45.8 ± 7.3	35.8 ± 6.4			
Chi Square	0.895	0.571	0.693			
DOF	12	11	11			
COARSE						
LDV-U-SS	ND	ND	ND	ND	ND	ND
LDV-L-SS	5.9 ± 3.2	7.1 ± 3.9	6.6 ± 3.6	22.6 ± 13.6	43.8 ± 28.9	42.6 ± 23.2
LDV-D-SS	ND	ND	ND	ND	ND	ND
Tire	8.9 ± 1.8	8.1 ± 1.7	7.2 ± 1.4	34.6 ± 10.6	50.1 ± 21.0	46.5 ± 9.0
Brake-Abs.	ND	ND	ND	ND	ND	ND
Brake-SM	3.5 ± 0.5	3.2 ± 0.5	1.6 ± 0.3	13.6 ± 3.7	19.7 ± 7.8	10.3 ± 1.9
T. Road Dust	17.9 ± 1.3	16.6 ± 1.4	7.0 ± 0.8	69.2 ± 16.8	103 ± 38	45.2 ± 5.2
Total	36.3 ± 4.0	35.0 ± 4.5	22.5 ± 4.0	140 ± 36	216 ± 83	145 ± 26
Measured	25.9 ± 6.0	16.2 ± 5.9	15.5 ± 4.7			
Chi Square	1.287	1.333	1.873			
DOF	12	11	11			

57

4.4.2 Source Contributions

The following seven source profiles were used in the CMB analysis of the tunnel aerosol chemistry:

LDV-U-SS: Light duty vehicle, unleaded gasoline, steady state

LDV-L-SS: Light duty vehicle, leaded gasoline, steady state

LDV-D-SS: Light duty vehicle, diesel, steady state

Tire: Tire wear based on the composition of tire rubber

Brake-Abs: Asbestos brake wear based on composition of brakes

Brake-SM: Semi-metal brake wear based on the composition of dust deposited on wheels, does not include composition of all semi-metal brake pads

T. Road Dust: Tunnel road dust

Heavy duty diesels were not considered because the organic and elemental carbon content of the steady state samples had not been determined due to limited resources. The federal test procedure profiles for heavy duty diesel vehicles, however, were reasonably similar and the LDV-D-SS profile is expected to provide a good estimate of the total diesel contribution.

The LDV-U source contribution could not be resolved from the other sources in either the fine or coarse particle size fractions. In addition, the diesel and asbestos brake impacts could not be resolved from the coarse particle size fraction.

An example of the CMB results are illustrated in Table 18 and Figure 8. The top portion of Table 18 describes the sample and provides a list of the fitting parameters. The next section lists the source contributions and their uncertainties. The bottom portion of the table lists the measured and calculated concentrations and their ratios.

Table 18

CMB RESULTS OF NET TUNNEL AEROSOL
FOR THURSDAY AM SAMPLING

SAMPLE ID: THAMF   THAMF   PARTICLE SIZE: FINE
FIELD FLAG: MASS FLAG: ANALYSIS FLAGS:
SITE: 1   Sepulveda Tunnel
SAMPLE DATE: 860925 START TIME: 6.8 DURATION: 3.2 HOURS
REDUCED CHI SQUARE: .895 DEGREES OF FREEDOM: 11

```
        --SOURCE----SIZE----UG/M3------------PERCENT---
        5398  LDL SS F   6.953+- 1.080   13.045+- 2.939
        5400  LDD SS F  26.225+- 5.517   49.202+-13.101
        5058  TIRE    T  10.200+- 1.970   19.137+- 4.839
        5472  BRAKE1  T   1.817+- 1.838    3.408+- 3.493
        5473  BRAKE2  T   2.382+-  .262    4.469+-  .880
        5466  TNNLRD  F   2.170+-  .934    4.071+- 1.875
        ------------------------------------------------
        TOTAL:    49.746+- 6.309   93.332+-19.292
```

--SPECIES		--MEAS. UG/M3--	--%--	--CALC. UG/M3--	--CALC./MEAS.--	
Al	*	.421+- .096	.789	.207+- .093	.491+- .249	Al
Si	*	.654+- .085	1.227	.713+- .101	1.090+- .209	Si
P	*	.149+- .036	.280	.068+- .032	.455+- .241	P
S	*	.406+- .227	.762	.311+- .162	.766+- .586	S
Cl	*	.310+- .099	.581	.175+- .103	.566+- .378	Cl
K	*	.019+- .013	.035	.032+- .009	1.726+-1.320	K
Ca	*	.152+- .021	.286	.127+- .045	.833+- .318	Ca
Ti	*	.012+- .007	.022	.013+- .002	1.143+- .704	Ti
V		< .003		.001+- .001	.000+- .000	V
Cr		.004+- .003	.007	.002+- .001	.693+- .745	Cr
Mn	*	.063+- .008	.118	.095+- .122	1.510+-1.948	Mn
Fe	*	1.227+- .140	2.303	1.228+- .093	1.000+- .137	Fe
Ni		.005+- .002	.010	.001+- .001	.249+- .186	Ni
Cu	*	.056+- .007	.105	.058+- .004	1.037+- .154	Cu
Zn	*	.125+- .015	.234	.131+- .012	1.046+- .160	Zn
Ga		< .004		.003+- .002	1.601+-4.251	Ga
As		< .067		.013+- .035	.000+- .000	As
Se		< .002		.000+- .001	.000+- .000	Se
Br	*	.803+- .092	1.507	.722+- .142	.898+- .205	Br
Rb		< .011		.000+- .005	.000+- .000	Rb
Sr		< .004		.006+- .001	.000+- .000	Sr
Y		< .006		.000+- .002	.000+- .000	Y
Zr		< .021		.002+- .005	.000+- .000	Zr
Mo		< .016		.009+- .003	.576+- .631	Mo
Pd		< .013		.000+- .003	.000+- .000	Pd
Ag		< .017		.000+- .004	.000+- .000	Ag
Cd		< .023		.000+- .006	.000+- .000	Cd
In		< .029		.000+- .007	.000+- .000	In
Sn		< .035		.016+- .009	.000+- .000	Sn
Sb		< .076		.000+- .019	.000+- .000	Sb
Ba	*	.171+- .041	.320	.101+- .044	.591+- .291	Ba
La		< .263		.000+- .065	.000+- .000	La
Hg		< .003		.000+- .001	.000+- .000	Hg
Pb	*	1.142+- .136	2.143	1.265+- .231	1.108+- .242	Pb
OC	*	19.780+- 3.370	37.111	21.221+- 1.656	1.073+- .201	OC
EC	*	20.480+- 2.910	38.424	19.512+- 2.808	.953+- .193	EC

```
-------------------------------------------------------------
```

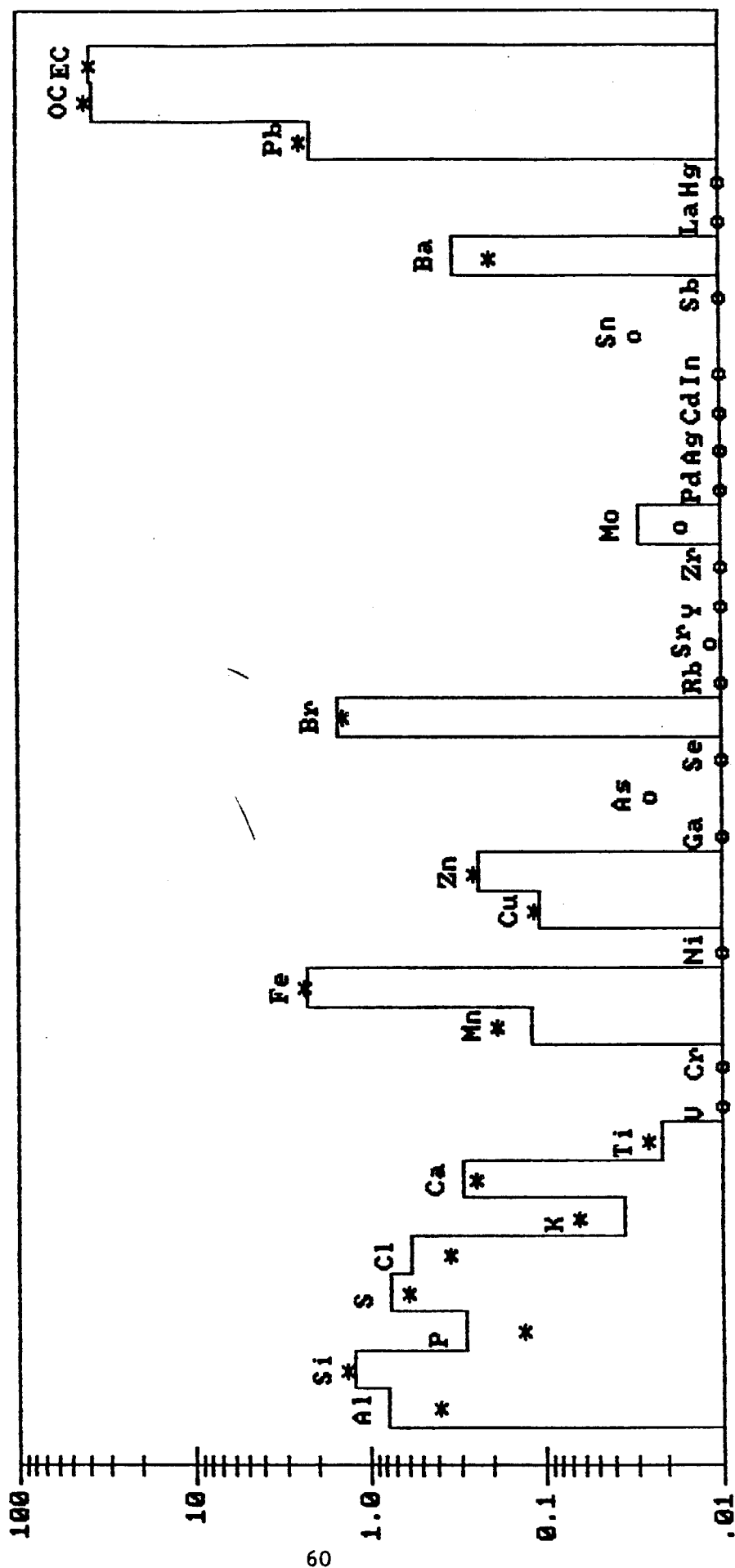MASS   53.3 +- 8.7   * FITTING SPECIES

Figure 8. Histogram plot (line ——) of the net tunnel aerosol chemistry after background subtraction on Thursday morning. The asterisks (*) indicate the calculated concentration of fitting species, and the open circles (0) indicate the calculated concentrations for the species not included in the least square regression calculation.

60

In this particular example, 93.3% of the Thursday morning fine particle mass was explained with the sources used. The uncertainty in the Brake 1 (Brake Abs.) category is slightly greater than its contribution and under some protocols might have been eliminated from the fit. It has been left in this fit primarily because it was close to the uncertainty, but also because it is known to be present in the aerosol. The inclusion of the LDV-U-SS profile in the CMB fit resulted in a negative contribution for this source. As a result, it was not included in any of the CMB fits.

The ratio of the calculated to measured elemental concentrations are generally equal to 1.0 within their standard deviations. It is not too surprising, however, that some elements are not fit as well because of potential limitations in source profiles such as tire and brake wear emissions. The chi square is reasonably good but is primarily influenced by the large uncertainties associated with the tailpipe emissions.

The quality of the fit can be more readily visualized with the histogram plot shown in Figure 8. The solid line represents the measured tunnel aerosol concentration. The asterisks show the model calculated concentrations of the elements used in the regression analysis. The open circles show the model calculated concentrations of the floating elements or elements not used in the regression analysis. In this example, it is clear that Si, Fe, Cu, Zn, Br, Pb, OC, and EC fit quite well while Al, P, S, Cl, Ca, Mn, and Ba are underfit, and K and Ti are overfit but still within one standard deviation of 1.0.

The fine particle road dust contribution was reasonably constant over the three sampling periods averaging 4.6% or 2.1 $\mu g/m^3$. The relative uncertainty in this contribution, however, was about 40%. The coarse particle contribution was much higher but showed a larger degree of variability. The first two sampling periods on Thursday showed road dust contributions of 17.9

and 16.6 $\mu g/m^3$, but dropped to only 7.0 $\mu g/m^3$ on Sunday.
One possible explanation for this large drop in the road dust
contribution might be associated with the rain early Thursday
morning which stopped just before our first sampling period. It is
possible that the rain mobilized road dust which was aerosolized
when the road dried. The road surface outside the tunnel had not
dried completely until shortly after the first sampling period had
started. Most of the road inside the tunnel was dry even during the
first part of the first sampling period. The Si background to
tunnel ratio showed a similar high degree of variability over the
three sampling periods ranging from 0.088 and 0.113 during the first
and second sampling periods on Thursday to 0.374 on Sunday. The
ratio of fine to coarse road dust contributions on Thursday of
0.12 ± 0.05 is close to the ratio obtained in the laboratory
resuspension of tunnel road dust, but the ratio of 0.26 ± 0.10
obtained on Sunday is high even when the uncertainty is taken into
account.

The percent mass explained in the coarse particle
fraction is substantially more than 100%, but on the average was
within 1.4 standard deviations of 100%. This over-explanation of
the coarse particle mass is thought to be due to the loss of sea
salt particles in the tunnel and large uncertainties in the net mass
after subtracting the background and tunnel road dust contributions.
The contribution attributed to the light duty vehicles using leaded
gasoline is also thought to be significantly over-estimated. The
road dust contribution is not thought to contribute significantly to
the over-explained coarse particle mass because of the large number
of reasonably unique species associated with this source and the
high quality of the CMB fits. In addition, the fine to coarse road
dust contribution ratios are consistent with the observed source
fine to coarse particle mass ratios.

The largest vehicle generated source contribution was
diesel exhaust. Its average PM_{10} impact was about 23 $\mu g/m^3$

based on its average fine particle contribution and fine to coarse particle ratio. Although this source category includes both light and heavy duty diesel vehicles, the total diesel source contribution should not be affected due to the high degree of similarity in the two diesel profiles.

Tire wear was the next largest source contribution to PM_{10} levels at 17 $\mu g/m^3$, followed by light duty vehicles using leaded gasoline.

One of the more precisely defined source contributions was semi-metal brake wear (BRAKE2) which had an average relative uncertainty of only 13% in the fine particle size fraction, and 16% in the coarse particle size fraction. This source was responsible for an average of 4.6% of the fine particle mass and 14.5% of the coarse particle mass. The fine particle semi-metal brake wear represented 43% of the total semi-metal brake wear which is quite close to the 45% obtained by Cha, et al, for asbestos brakes (51). The ratio of semi-metal to asbestos brake contributions is hard to evaluate because of limited available information. Indications from new car dealers and parts suppliers are that this level of impact is reasonable based on the significantly higher wear rate of the semi-metal brake pads and the large fraction of new cars using them.

The large tire wear contribution relative to the other source contributions was surprising at first because previous authors (44,46) indicated its contribution was small. However, the conclusions reached by these previous investigators was based on measurements over ten years ago when emissions from vehicles using leaded gasoline were higher and LDV-L represented a much larger fraction of the vehicle fleet. The relatively large tire contribution is consistent with estimated emission rates as discussed in the following subsection.

4.4.3 Emission Rates

Emission rates were calculated based on rough estimates of the tunnel ventilation flow rate, measured vehicle miles traveled, and source contribution estimates developed from the CMB analysis. The details of the calculations are presented in Appendix R. The general theory used to calculate the emission rates from tunnel measurements was discussed in Section 2.0 of this report, but is summarized below in more convenient terms.

The emission rate, E, is given by the following general equation:

$$E = F \cdot t \cdot S \div T$$

where

F = average flow rate of ventilation air, m^3/min

t = sampling interval, min

S = source contribution, $\mu g/m^3$

T = vehicle miles traveled (VMT)

The ventilation flow rate was estimated from an evaluation of the ventilation air velocity leaving the tunnel exit and the vent duct exits at the time of the experiment. Only half of the ventilation was considered since the vehicle count considered only half of the traffic flow. The tunnel ventilation relied primarily on winds and ventilation from the ram effect of vehicles entering the tunnel. It was estimated that the average velocity of air exiting the tunnel was about 8 mph through an area of about 800 ft^2. Air also exited the tunnel through two air vents at each end of the tunnel. It was estimated that the velocity of air through each of these ducts was about 15 mph through an area of about 64 ft^2. The total air flow through the ducts and tunnel based on these estimates was about 21,000 m^3/min.

Emission rates were calculated based on the above rough estimates of ventilation flow rate, the source contributions listed in Table 17, VMT and sampling times listed in Table 3. The results are summarized in Table 19.

The average emission rate for all sources in the tunnel was about 105 mg/mi. After subtracting the emission rate of tunnel road dust, the net emission rate due to vehicle emissions was about 80 mg/mi. The diesel emission rate calculated from these tunnel estimates is about 1000 mg/mi. This is in good agreement with the weighted average emission rate for light and heavy duty diesel vehicles. For example, the light duty diesel emission rate in our steady state tests was 313 mg/mi (Table 6). Pierson and Brachaczek reported an emission rate of 1392 ± 160 mg/mi. for heavy duty diesels in tunnels (22). Weighting these emission rates in proportion to the VMT by these two categories yields an emission rate of 761 mg/mi, which is in reasonably good agreement with our tunnel derived estimate of 1000 mg/mi.

The average tunnel calculated tire wear emission rate of 28 mg/mi is also in good agreement with the literature value of 20 ± 12 (44-47).

The semi-metal brake wear contribution is substantially less than the values reported in the literature (50,51). The largest source of uncertainty in this emission factor other than the tunnel flow rate is the unknown number of vehicles using this type of pad. If all of the vehicles were using this type of brake, the emission rate would be about 7.7 mg per vehicle mile. This is about half the emission rate of 12 mg/mi reported by Cha, et al, for asbestos brake pads assuming four brake pads per vehicle (51). Semi-metal brake pads are commonly used only on front wheel disk brakes in which case the asbestos brake emission rate applied to semi-metal brakes would be only 6 mg/mi. It is assumed, however, that semi-metal brake pads are not used on all vehicles and on those

Table 19

ESTIMATE OF AVERAGE PM_{10} VEHICLE EMISSION RATES
BASED ON TUNNEL MEASUREMENTS[a]

Source Category	Emission Rate (mg/vehicle mile)
Average Total Tunnel Emissions[b]	105
Tunnel Road Dust[b]	25
Net Vehicle Emission Rate[b]	80
LDV-D-SS[c]	1000
Tire Wear[b]	28
LDV-L-SS[c]	172
Semi-metal Brake Wear[b]	7.7
LDV-U-SS	?
Asbestos/Organic Brake Wear	?

a. Details of calculations are provided in Appendix R

b. Based on total VMT in southbound lane

c. Emission rates per source category mile

vehicles using this type of pad, it is further assumed that they are used only on the front disk brakes. In this case, the emission rate per brake mile would be substantially greater than that for asbestos brakes.

The calculated emission rate for light duty vehicles using leaded gasoline was 172 mg/mi, which is fourteen times greater than the SS tailpipe tests of 12.4 mg/mile from Table 6. The fine particle tailpipe tests for this vehicle category were, in fact, the most reproducible and exhibited some of the smallest relative standard deviations. The coarse particle profile was much more uncertain but represents only about 15% of the emission rate. For this source and the diesel emission rate calculations, only the fine particle emission rate was calculated from the source impacts. The PM_{10} emission rate was based on the fine to coarse particle emission ratios rather than the source contributions to the coarse particle tunnel aerosol. It is expected that the source contributions to the fine fraction is reasonably accurate based on the excellent fitting of the Mn, Br, and Pb concentrations. The largest potential uncertainty would be associated with the tunnel flow rate, but it must be the same for all source categories, and it is unlikely that it would be ten fold too low. A more likely source of error is the VMT by vehicles using leaded gasoline. This calculation was based on a 1975 model year cut point for catalyst equipped vehicles, but it also is not expected to be low by ten fold. Another source of uncertainty might be in how the medium and heavy duty vehicles using leaded gasoline were counted, and the emission rate for these categories. At this time, explanation of the high emission rate for this source category is unknown.

The CO concentrations measured in the tunnel during our three sampling periods are compared in Table 20 to the CO concentrations calculated from CO emission rates listed in Table 6. The calculated and measured emission rates are in reasonably good agreement for the first sampling period, but in poor agreement for

Table 20

COMPARISON OF MEASURED TUNNEL CARBON MONOXIDE CONCENTRATIONS
WITH CALCULATED CONCENTRATIONS

Sampling Period	CO (mg/m^3)	
	Measured	Calculated
Thursday, AM	3.6	2.7
Thursday, PM	21.7	2.8
Sunday	7.2	1.7

the other periods. Although the agreement is best on the first day, the difference in the background and tunnel concentrations were surprisingly small. The tunnel samples on the other days, however, were questionable because of the hose separation. Strong conclusions cannot be drawn from these CO comparisons because of these uncertainties in the data.

It needs to be emphasized that the emission rates are based on very rough estimates of tunnel flow rates. Because of this, the excellent agreement between tunnel estimated emission rates and emission rates based on either our tailpipe measurements or literature values must be considered somewhat fortuitous. The more important result is the consistency of the relative emission rates except for the vehicles using leaded gasoline.

4.4.4 Source Contributions to Tunnel Aerosol Constituents

Source contributions to the net tunnel aerosol mass were used to calculate the contribution each source makes to selected aerosol constituents. The results of these calculations are summarized for fine and coarse particles in Table 21. The contribution that light duty vehicles using unleaded gasoline make to both the fine and coarse particles is not included because this source was not resolved. The contribution vehicles using diesel fuel and asbestos brakes make to the tunnel aerosol also could not be determined in the coarse particle fraction.

All of the fine particle organic carbon was explained with the five sources listed. Vehicles using diesel fuel contributed 57.5% of the organic carbon, and tire wear was responsible for 30.1%. Vehicles using unleaded gasoline could not be resolved, but are probably responsible for a significant portion of the organic carbon.

Table 2I

SOURCE CONTRIBUTIONS TO SELECTED SPECIES IN TUNNEL AEROSOL*
(Percent)

– Fine Particle Fraction –

Element	R. Dust	LDV-L	Source Category LDV-D	Tire Wear	Asb. Brakes	SM Brakes	Explained
OC	1.5 ± 0.8	18.2 ± 4.5	57.5 ± 15.8	30.1 ± 10.9	0	0	107 ± 24
EC	0.19 ± 0.10	0.45 ± 0.36	80.35 ± 24.06	14.29 ± 6.05	0	0	95 ± 26
Al	36.6 ± 17.9	11.1 ± 22.3	0.56 ± 0.64	< 0.02	0.93 ± 1.0	< 0.01	49 ± 29
Si	59.2 ± 26.8	16.9 ± 14.0	2.1 ± 2.3	0.8 ± 0.8	30.0 ± 31.2	< .01	109 ± 45
K	106 ± 88	49 ± 55	17.7 ± 26.0	< 0.5		< 0.1	172 ±
Ca	47.5 ± 21.6	4.6 ± 5.3	4.0 ± 5.0	3.3 ± 2.2	23.8 ± 37.6	< 0.02	83 ± 45
Ti	95 ± 70	1.6 ± 5.1	0.2 ± 2.0	17.3 ± 20.4	< 0.2	< 0.2	114 ± 81
Mn	2.5 ± 1.1	148 ±	< 0.4	0.08 ± 0.05	< 0.03	< 0.04	151 ±
Fe	6.5 ± 2.9	0.1 ± 0.2	0.04 ± 0.09	< .01	4.3 ± 4.4	89 ± 16	100 ± 18
Ni	5.7 ± 3.6	19.2 ± 16.7	< 3.6	< 2.0	0	< 0.5	24.9 ± 19.0
Cu	3.0 ± 1.3	3.9 ± 1.7	0.8 ± 0.9	0.09 ± 0.09	0	96 ± 18	104 ± 19
Zn	4.6 ± 2.1	6.1 ± 2.0	7.8 ± 5.0	82	4.5 ± 5.5	0	105 ± 23
Br	0.06 ± 0.03	89.7 ± 24.7	0.06 ± 0.09	0.01 ± 0.01	0	0	90 ± 25
Ba	1.2 ± 0.9	< 19	< 8	< .06	9.8 ± 18	48 ± 13	59 ± 31
Pb	0.7 ± 0.3	110 ± 29	0.6 ± 0.8	0	0	0	111 ± 30

– Coarse Particle Fraction –

Element	R. Dust	LDV-L	Source Category Tire Wear	SM Brakes	Explained	Coarse**
OC	27.8 ± 6.9	9.8 ± 13.7	63 ± 25	0	101 ± 34	29
EC	5.14 ± 2.26	4.14 ± 20.16	127 ± 74	0	136 ± 80	9
Al	99.1 ± 15.7	3.0 ± 5.4	< 0.01	< 0.01	102 ± 17	76
Si	81.1 ± 12.4	0.25 ± 0.33	0.10 ± 0.10	< 0.01	81.5 ± 12.5	88
K	135 ± 29	0.8 ± 1.2		< 0.02	136 ± 30	92
Ca	79.2 ± 13.0	1.3 ± 2.0	0.6 ± 0.4	< 0.01	81 ± 13	82
Ti	132 ± 38	0.5 ± 4.3	2.1 ± 2.2	< 0.04	134 ± 39	88
Mn	38.2 ± 6.4	36.3 ± 49.7	0.09 ± 0.06	< 0.07	74.6 ± 50.6	44
Fe	33.9 ± 5.1	0.1 ± 0.2	< .01	55.4 ± 11.5	89 ± 15	70
Ni	15.1 ± 3.9	11.5 ± 13.0	< 0.9	< 0.3	26.6 ± 14	67
Cu	21.4 ± 4.2	0.8 ± 1.0	0.06 ± 0.06	100 ± 24	123 ± 27	59
Zn	31.8 ± 4.8	3.2 ± 4.1	59 ± 15	0	94 ± 18	55
Br	11.5 ± 2.9	212 ±	0.23 ± 0.20	< 0.09	223 ±	5
Ba	11.4 ± 3.4	< 6.9	< .04	48 ± 15	59 ± 19	60
Pb	22.1 ± 3.6	62 ± 65	< .03	0	85 ± 65	23

Thursday morning

* Percent of PM_{10} mass in coarse particle size fraction

70

Vehicles using diesel fuel were responsible for 80% of the fine particle elemental carbon, while tire wear contributed only 14%. Other sources contributed less than 0.5%.

Tire wear was responsible for most of the coarse particle organic and elemental carbon. Although road dust contributed 27.8% of the organic carbon, most of it is thought to be of vehicle origin. Microscopic analysis of resuspended tunnel dust indicated that a substantial portion of the coarse particles appeared to be tire wear products. The high organic carbon to elemental carbon ratio in the coarse particle road dust profile, however, is inconsistent with this microscopic analysis. It does suggest that the organic to elemental carbon ratio in the tire wear profile of 2:1 is too low.

Almost all of the Al, Si, K, Ca, and Ti originates from the road dust, about 90% of which consists of coarse particles. Although 99% of the coarse particle Al was due to this source, only 81% of the Si was due to the tunnel road dust. None of the other coarse particle sources accounted for more than 0.25% of the Si. The 18% unexplained coarse particle Si was most likely associated with asbestos type brake pad wear. The asbestos brake wear also emits substantial amounts of Ca, the other crustal element for which only about 80% of the mass was explained. Based on the fine particle asbestos brake contribution, much of the unexplained Ca could be due to brake wear.

Only 50% of the fine particle Al is explained by the five fitting sources, 37% of which was from road dust and 11% from vehicles using leaded gasoline. It is uncertain at this time what is responsible for this unexplained Al.

All of the fine particle Si was explained with the five fitting sources, 90% of which was due to road dust and asbestos brake wear. Asbestos brakes were responsible for 30% of the Si and

24% of the fine particle Ca, the other major source of which was road dust. Fine particle K and Ti was dominated by the road dust source, although the two exhaust sources were responsible for a significant portion of the K.

Sources of Mn and Fe have typically been associated with road dust. However, vehicles using leaded gasoline were a significant source of Mn, and semi-metal brake pads were a significant source of Fe. In addition, almost all of the Cu was from semi-metal brakes. Nickel is also thought to be associated with these semi-metal brake pads, even though it was not apportioned to this source. The semi-metal brake source profile is based on one sample which didn't contain Ni. Other brake pads analyzed semi-quantitatively indicated the presence of Ni. In support of this is the fine to coarse ratio for Ni which is in sharp contrast to historical ambient measurements when residual oil combustion was the dominant source of Ni. These results, in which 67% of the Ni is in the coarse particle fraction, is consistent with the previously reported asbestos brake wear pattern and the measured semi-metal brake wear in this study. Almost all of the Ba has also been apportioned to brake wear. A substantial portion of both the fine and coarse particle fractions is unexplained, but is thought to be due to brake wear profile limitations.

Zinc is about equally distributed between the fine and coarse particles, with almost all of the fine particle Zn (82%) being explained by tire wear. Tire wear was responsible for 59% of the coarse particle Zn, and road dust explained 32% of the Zn. Much of the Zn in the road dust may be due to tire wear products, but semi-metal brake wear may contribute to this element based on the semi-quantitative analysis results presented in Table 16. Zinc is enriched in all of the SCAB paved road dust samples relative to airshed soil samples. In all cases, the Zn left over after subtracting the soil Zn can explain most of the measured coarse particle carbon based on the tire profile, but the road dust OC/EC ratio is in sharp disagreement with the literature.

All of the fine particle Br and Pb came from vehicles using leaded gasoline. Most of the coarse particle Br and Pb also came from this source, but a sizable fraction came from road dust.

4.4.5 Composite Tunnel Vehicle Emissions Profile

A composite tunnel vehicle emissions profile was calculated by subtracting the road dust contribuion to each of the measured species. The resulting profiles are listed in Table 22 and illustrated in Figure 9. Ninety-eight percent of the fine particle mass is explained with the fine particle species and their assumed oxides. The coarse particle profile, however, is a normalized profile which was necessary because of the large error in the net coarse particle mass caused by the loss of marine aerosol in the tunnel. The coarse particle profile was developed by first averaging the concentration ratios to Pb for the three sampling periods, assuming typical compounds and normalizing to 100%. This final normalizing factor was then used to adjust the elemental concentrations to the values reported in Table 22. The PM_{10} profile could not be calculated because of the errors in the coarse particle mass caused by the loss of marine aerosol.

The fine particle profile is dominated by organic and elemental carbon of about equal concentrations originating mostly from diesel exhaust and tire wear. Iron, Br, and Pb are the next most abundant elements which are associated with brake wear (Fe) and use of leaded gasoline (Br, Pb).

The coarse particle profile is dominated by species contributed by tire and brake wear and exhaust from vehicles using leaded gasoline. The Si to Ca ratio of 4.6 in this profile is consistent with the 5.7 ratio reported by Ondov (34) for asbestos brake wear in Table 14. It is important to note that the net Zn concentration in both the fine and coarse particle fractions is about two times greater than the Cu concentration. This, along with

Figure 9

TUNNEL ON-ROAD MOTOR VEHICLE

Table 22

P E R C E N T   C O M P O S I T I O N

SPECIES	FINE		COARSE		TOTAL
Al	.3377 +-	.1307	.8160 +- 2.1543		
Si	.3827 +-	.2245	6.0532 +-14.0863		
P	.2929 +-	.0536	.2405 +- .5216		
S	.7314 +-	.3035	.0920 +- 1.6431		
Cl	.3631 +-	.3242	.0000 +-20.7482		
K	.0193 +-	.0210	.0000 +- .7843		
Ca	.1250 +-	.0480	1.3272 +- 2.7186		
Ti	.0041 +-	.0111	.0082 +- .1319		
V	.0000 +-	.0038	.0000 +- .0686		
Cr	.0044 +-	.0039	.0184 +- .0473		
Mn	.1340 +-	.0171	.2008 +- .4262		
Fe	2.2183 +-	.2765	11.3379 +-23.0810		
Ni	.0096 +-	.0028	.0559 +- .1106		
Cu	.1118 +-	.0143	.2909 +- .6112		
Zn	.2465 +-	.0307	.6064 +- 1.1496		
Ga	.0027 +-	.0051	.0033 +- .0117		
As	.0390 +-	.0817	.0000 +- .1080		
Se	.0000 +-	.0024	.0023 +- .0070		
Br	1.3551 +-	.1644	.2688 +- .6335		
Rb	.0000 +-	.0110	.0176 +- .0500		
Sr	.0000 +-	.0054	.0000 +- .4804		
Y	.0000 +-	.0078	.0000 +- .0145		
Zr	.0000 +-	.0258	.0000 +- .0654		
Mo	.0195 +-	.0179	.0389 +- .0617		
Pd	.0000 +-	.0159	.0000 +- .0365		
Ag	.0000 +-	.0208	.0000 +- .0479		
Cd	.0000 +-	.0275	.0000 +- .0639		
In	.0000 +-	.0345	.0000 +- .0797		
Sn	.0000 +-	.0418	.0000 +- .0963		
Sb	.0000 +-	.0918	.0000 +- .2155		
Ba	.3282 +-	.0560	1.0768 +- 1.9048		
La	.0000 +-	.3176	.0000 +- .7222		
Hg	.0000 +-	.0031	.0016 +- .0070		
Pb	2.4366 +-	.2975	2.0488 +- 3.9517		
OC	38.5859 +-	5.5504	39.1636 +-61.7037		
EC	38.1189 +-	4.9093	12.6561 +-24.2750		
Sum	85.8667		76.3252		

the data in Tables 15 and 16, suggests that most of the Zn is contributed by tire wear and not semi-metal brake pad wear which is supportive of the tire wear contribution.

It needs to be emphasized that these composite profiles represent only the vehicle fleet and operating conditions during the time of our sampling period. Our original thought was that the tunnel composite profiles would be representative of steady state conditions with minimal contributions from tire and brake wear. Because of the partial tunnel lighting failure on Thursday, braking was significant, followed by an acceleration. This makes these results more difficult to compare with a composite source profile calculated from the individual steady state source profiles. Although the braking and acceleration adds characteristics to the operating conditions that are typical of the air basin, the degree to which these operating features add to the profiles is unpredictable.

4.5 Exhaust Composite Vehicle Emission Profiles (MOVES)

4.5.1 Overview

Sources which are either collinear with other sources or have relatively non-descriptive profiles cannot be quantified as individual source categories in a CMB analysis. Their impacts, however, can in some cases, be estimated by using either emission inventory scaling after a CMB analysis or by developing a composite source profile based on emission inventory scaling before the CMB analysis.

One requirement is that the unresolved sources have similar emission and dispersion characteristics to those of a source that can be quantified. If this is the case, then the unresolved source contribution can be estimated from the resolved source by the ratio of their total airshed emissions rates. In emission inventory

scaling, the ratio is applied after the CMB analysis. Omitting the source that cannot be resolved in the CMB analysis, however, can alter the fitting process if some of its constituents contribute significantly to any of the species used in the CMB regression analysis.

If individual source profiles are available for both the resolved and unresolved sources, then this problem can be avoided by developing a composite source profile based on the same relative emission inventory ratios. The advantage to this latter procedure is that it includes the chemical constituents from all sources in the source profile. The disadvantage is that the resulting profile depends on relative emission rates, which is one of the main disadvantages of dispersion modeling. That is, in normal CMB analysis, source contributions depend only on the relative source composition chemistry, not emission rates. In developing a composite source profile for sources that might otherwise not be resolved, the resulting profiles depend on the relative emission rates. If these emission rates are not well known, then the resulting profile can limit the accuracy of both source contributions.

Emissions from vehicles using unleaded gasoline and diesel fuel, as well as tire wear and asbestos brake wear, are examples of sources that have been difficult to resolve on an individual basis. Although the diesel and tire wear were relatively easily resolved in the tunnel, they typically have not been resolved in the ambient environment because of the presence of emissions from other sources and the fact that some species such as S and OC cannot be used in the fitting because of significant contributions from secondary particles. In addition, the contributions from tire and brake wear were previously thought to be insignificant. The results of this work clearly show a shift in the relative importance of source categories and have dictated a re-evaluation of the type of composite profile required.

In this study, several composite source profiles have been developed using NEA's MOVES Program (Appendix A). These composite profiles are grouped into profiles based on steady state tailpipe emission profiles for comparison with the tunnel results and profiles based on federal test procedures for use in the SCAB.

4.5.2 MOVES

The MOVES program is designed to develop a composite source profile for motor vehicle emissions based on individual source emission profiles, emission factors (mg/mi), VMT, and the average lead in leaded gasoline. Emission rates are calculated, relative weighting ratios determined, and a weighted average profile determined. If the average lead in leaded gasoline has changed from the base year that the profile was developed, the program will modify the leaded gasoline profile accordingly before forming the composite profile. The program can form a composite profile from light and heavy duty vehicles using unleaded, leaded, and diesel fuels, as well as tire and brake wear. The details of this program are described in Appendix A.

4.5.3 Emission Factors and VMT

The emission factors and VMT used to calculate composite source profiles representing tunnel and SCAB conditions are summarized in Table 23. The tunnel VMT are those based on the vehicles using the tunnel during each of our sampling periods. The emission factors (mg/vehicle mile) for exhaust emissions are based on our steady state tailpipe measurements. The heavy duty diesel emission rates are based on the tunnel results of Pierson, et al (22). The tire wear emission rates are based on a composite of the values reported in AP42 (49), Cardina (47), Cadle (46), and Pierson (44,45) Brake emission rates for vehicles traveling at a steady speed are not available. Although one would not expect emissions from brakes when the brakes are not being applied, it is reasonable

78

Table 23

SUMMARY OF EMISSION FACTORS AND VEHICLE MILES TRAVELED
USED TO CALCULATE COMPOSITE SOURCE PROFILES

TUNNEL STUDY (Steady State)

Vehicle Type	Vehicle Miles Traveled[a]			Emission Factors (mg/vehicle mile)[a]		
	THAM	THPM	SUAM	Fine	Coarse	PM10
LDV-U	2386 ± 119	3257 ± 163	2008 ± 100	4.3 ± 7.8	0.70 ± 0.16	5.0 ± 7.9
LDV-L	181 ± 9	229 ± 11	133 ± 7	10.1 ± 5.0	2.3 ± 2.0	12.4 ± 5.3
LDV-D	56 ± 2	76 ± 4	47 ± 2	298 ± 218[d]	15.4 ± 8.3	313 ± 225
HDV-D	48 ± 2	44 ± 2	35 ± 2	1322 ± 160[d]	70 ± 200[d]	1392 ± 160[d]
Tires	-	-	-	16 ± 8[e]	16 ± 8[e]	32 ± 16[e]
Brakes-A	-	-	-	-	-	-
Brakes-M	-	-	-	-	-	-

SOUTH COAST AIR BASIN
(Federal Test Procedure)

Vehicle Type	Vehicle Miles Traveled(X10⁻⁶)[b]	Total Exhaust[b] Emissions(T/D)	Total Tire[b] Emissions(T/D)	Emission Factors (mg/vehicle mile)[b]				
				Exhaust[b]	Tires[b]	Fine	Coarse	PM10
LDV-U (C)	140.6	9,800	30.9	63.2	199	7.6± 4.9	1.8± 0.5	9.3± 4.9
LDV-L (NC)	43.7	18,200	10.1	378	210	97.6±76	37.6±63	135 ±135
LDV-D	5.1	2,200	1.1	391	195	2186±2149	110±60	2297±2209
HDV-D	7.4	20,200	5.4	2480	662	-	-	-
Tires						16±8[e]	16±8[e]	32±16[e]
Brakes-A[c]						5.6±2.8	6.9±3.4	12.5±6.2
Brakes-M						-	-	-

a. This work, steady state, and federal test procedure
b. CARB predicted SCAB, VMT, and emission rates for 1985 in tons/day
c. Cha, et al, Ref. 51
d. Pierson, et al, assumed 95% < 2.5 μm, Ref. 22
e. AP42, Cardina, Cadle, Pierson, Ref. 44-46, 49

to expect some blow off of brake dust that had formed during the previous braking periods. In addition, even when all the lights in the tunnel were on as they were on Sunday, one would still expect some braking during normal tunnel use because of requirements to adjust speed for general traffic conditions. Because of the obvious large brake wear contributions observed in the tunnel and their large contributions to tunnel chemistry, the absence of these emission factors seriously limits the utility of the composite tunnel profiles for evaluating the compositing method.

The VMT in the SCAB are based on California Air Resources Board's (CARB) emission inventory estimates for 1985 (Appendix S). The emission factors are from several different sources. Exhaust and tire wear emission rates are based on the same CARB emission inventory. Exhaust emission factors from our FTP results are also listed, as well as tire wear emission rates from AP42 (49), Cardina (47), CadTe (46), and Pierson (44,45). The tire wear emission factors used in this latter case are similar to those used for the tunnel profiles. The asbestos brake wear factors are based on the work of Cha, et al (51). Emission factors for semi-metal brakes are not included. This is not thought to represent a significant problem, however, because the profile for this source category is such that it should be adequately resolved and quantified on its own.

4.5.4 Composite Source Profiles

Composite source profiles developed in this study are listed for two steady state and three federal test procedure combinations in the Source Profile Library in Volume II of this report. Source profile 0-01, MOVES-SS (NEA-E, WOB, T42, TVMT) is based on NEA's tailpipe emissions factors (NEA-E), without brake contributions (WOB), using the AP42 tire wear factors (T42), and the average tunnel VMT (TVMT), while the other profile, 1-02, is without brake and tire contributions.

The two composite tunnel profiles are generally in poor agreement with the measured tunnel profile. Part of this disagreement is due to the absence of the brake wear contribution, as well as the uncertainty in VMT by LDV-L. The ratio of the organic and elemental carbon concentrations in the fine particle fraction, however, is within two percent of the tunnel ratio. The percent concentration of these two species in the fine composite profile is about 12% higher than in the tunnel. The difference, however, would be reduced to about 6% if the brake wear component were included.

The differences of most significance are for those elements associated with leaded gasoline. The composite fine particle profile (0-01) concentration of Mn, Br, and Pb are about 5 to 7 times less than what was measured in the tunnel. This is consistent with the relatively high emission rate for vehicles using leaded gasoline determined from our tunnel measurements. The relative concentration of these three elements, like organic and elemental carbon, are in good agreement with the tunnel measurements.

The excellent agreement in the relative elemental chemistry and the relatively good quality of the CMB fits suggests that the tailpipe exhaust profiles are all good representations of the average tunnel profile. The profile differences observed are consistent with the omission of brake wear contributions and the possibility of more vehicles using leaded gasoline than had been predicted from the traffic count. It can be concluded from this, that if the appropriate VMT and emission factors were available for all of the sources, the measured exhaust profiles would yield a reasonably good calculated composite profile.

The three composite source profiles based on our FTP results are designed to represent the vehicle emission profile for the SCAB. A large number of such composite profiles could be

81

developed from a variety of combinations depending on which sources are included, emission factors used, etc. Only the three profiles most likely to be used are listed in the source profile library. Two of them include only vehicle exhaust emissions. It is thought that these profiles, plus a composite brake wear profile, along with a tire wear profile, might best resolve the influence of the vehicle emissions. A composite source profile, including tire and brake wear, is also included, but it doesn't include the semi-metal brake wear component.

5.0 CONCLUSIONS AND RECOMMENDATIONS

One of the primary conclusions of this study is that tire and brake wear emissions are much more significant than previously considered. Tire wear was the second largest source of particulates in the Sepulveda Tunnel, and equal to 75% of the largest impact source category, diesel exhaust.

Semi-metal brake pad wear was identified as a new source of vehicle emissions. The emission rates from this source are estimated to be substantially greater than emission rates from asbestos brake pads. This new category is the primary source of both fine and coarse particle Fe, Cu, and Ba and may contribute significant quantities of Mg, Al, Si, Cl, Ca, Mn, Ni, Zn, Sr, Mo, and Sn.

The magnitude of these source contributions relative to exhaust contributions has significantly affected the utility of a composite source profile for the SCAB that includes these sources.

Source profiles are provided for all of the major source categories, as well as composite source profiles based on tunnel measurements and calculated composite source categories for the tunnel and the SCAB.

The primary recommendation resulting from this study is to improve the source profiles for tire and brake wear emissions. In the meantime, vehicle emission impacts should be apportioned using one of the composite vehicle exhaust emissions profiles, along with composite profiles for tire wear and brake wear based on the current profiles. Emission rates and VMT for the whole air basin should be improved and new MOVES composite profiles calculated.

It is also recommended that the characteristics of the marine aerosol and its modification during transport be defined, and emission rates and profiles for emissions from electric motors, alternators, etc., be estimated.

6.0 REFERENCES

1. Air Resources Board, State of California Air Resources Board Emissions Inventory, 1979, prepared by the Stationary Source Control Division, Emission Inventory Branch, California Air Resources Board, Sacramento, CA, 1982.

2. Cass, G.R., P.M. Boone, and E.S. Macias, "Emissions and Air Quality Relationships for Atmospheric Carbon Particles in Los Angeles", Particulate Carbon, Atmospheric Life Cycle, edited by G.T. Wolff and R.K. Klimisch, Plenum Press, New York, 1982.

3. Chass, R.L., and R.E. George, "Contaminant Emissions from the Combustion of Fuels", J. of the Air Poll. Control Assn., 10, 34, 1960.

4. Dzubay, T.G., R.K. Stevens, and L.W. Richards, "Composition of Aerosols Over Los Angeles Freeways", Atmospheric Env., 13, 653, 1979.

5. Grisinger, J.E., "Air Quality Management Plan 1982 Revision: Appendix No. VI-C, Nitrogen Dioxide, Sulfur Dioxide and Sulfate Analyses for the South Coast Air Basin", South Coast Air Quality Management District, El Monte, CA, 1982.

6. Huang, A.H., and S.J. Head, "Estimation of Fugitive Hydrocarbon Emissions from an Oil Refinery by Inverse Modeling", Third Symposium on Fugitive Emissions: Measurement and Control, U.S. Environmental Protection Agency. (Also, Technical Paper TP8162, AeroVironment, Inc., Monrovia, CA). 1978.

7. Mayrsohn, H., and J.H. Crabtree, "Source Reconciliation of Atmospheric Hydrocarbons", Atmospheric Env., 10, 137, 1976.

8. Mayrsohn, H., J.H. Crabtree, M. Kuramoto, R.D. Sothern, and S.H. Mano, "Source Reconciliation of Atmospheric Hydrocarbons 1974", Atmospheric Env., 11, 189-192, 1977.

9. Oliver, W.R., and S.H. Peoples, "Improvement of the Emission Inventory for Reactive Organic Gases and Oxides of Nitrogen in the South Coast Air Basin", Volume One: Main Report, System Applications, Inc. Report No. SYSAPP-85/080, San Rafael, CA, 1985.

10. Parungo, F.P., R.F. Pueschel, and D.L. Wellman, "Chemical Characteristics of Oil Refinery Plumes in Los Angeles", Atmospheric Env., 14, 509-522, 1980.

11. Pitts, J.N., A.M. Winer, H.W. Biermann, and E.C. Tuazon, "Direct Measurements of Nitrous Acid, Nitrogen Dioxide and Formaldehyde in Auto Exhaust by Differential Optical Absorption Spectroscopy", California Air Resources Board Report No. Al-089-32, Sacramento, CA, 1984.

12. Pueschel, R.F., F.OP. Parungo, E.W. Barrett, D.L. Wellman, and H. Proulx, "Environmental Effects of Oil Refinery Operations in Los Angeles", NOAA Technical Memorandum APCL-22, Boulder, CO, 1979.

13. Richards, L.W., E.L. Avol, and A.B. Harker, "The Chemistry, Dispersion, and Transport of Air Pollutants Emitted from Fossil Fuel Power Plants in California: Ground Level Pollutant Measurement and Analysis, California Air Resources Board Report No. ARB-R-3-916-64, Sacramento, CA, 1976.

14. Richards, L.W., H.H. Wang, and A.B. Harker, "Motor Vehicles Sampling Experiment", California Air Resources Board Report No. ARB-R-335-77-73, Sacramento, CA, 1977.

15. Rodes, C.E., and D.M. Holland, "Variations of NO, NO_2, and O_3 Concentrations Downwind of a Los Angeles Freeway", Atmospheric Env., 15, 243-250, 1981.

16. Rose, A.H., R. Smith, W.F. McMichael, and R.E. Kruse, "Comparison of Auto Exhaust Emissions in Two Major Cities", J. of the Air Pollution Control Assn., 15, 362, 1965.

17. Taback, H.J., A.R. Brienza, J. Macko, and N. Bruentz, "Fine Particle Emissions from Stationary and Miscellaneous Sources in the South Coast Air Basin - Final Report", California Air Resources Board Report No. ARB-R-191-30-79-94, Sacramento, CA, 1979.

18. Core, J.E., J.J. Shah, and J.A. Cooper, "Receptor Model Source Composition Library", EPA-450/4-85-002, November, 1984.

19. NEA, Inc., 10950 S.W. 5th St., Suite 380, Beaverton, OR, 97005.

20. NEA, Inc., "PM_{10} Source Profile Library Development Plan for the South Coast Air Basin", final report to the South Coast Air Quality Management District, July 8, 1986.

21. Kittelson, D.B., and D.F. Dolan, "Dynamics of Sampling and Measurement of Diesel Engine Exhaust Aerosols", presented at the Conference on Carbonaceous Particles in the Atmosphere, Lawrence Berkeley Laboratory, University of California, Berkeley, CA, March 20-22, 1978.

22. Pierson, W.R., and W.W. Brachaczek, "Particulate Matter Associated with Vehicles on the Road.II", Aerosol Science and Technology, 2, 1, 1983.

23. Hering, S.V., A.H. Miguel, and R.L. Dod, "Tunnel Measurements of the PAH, Carbon Thermogram, an Elemental Source Signature for Vehicular Exhaust", The Science of the Total Environment, Vol. 36, June 1, 1984.

24. Gorse, R.A., and J.M. Norbeck, "CO Emissions Rates for In-Use Gasoline and Diesel Vehicles", Journal of the Air Pollution Control Association, 31, 1094, 1981.

25. Lonneman, W.A., R.L. Sella, and S.A. Meeks, "Non-Methane Organic Composition in the Lincoln Tunnel", Environ. Sci. Technol., Vol. 20, No. 8, 1986.

26. Hampton, C.V., W.R. Pierson, T.M. Harvey, W.S. Updegrove, and R.S. Marano, "Hydrocarbon Gases Emitted from Vehicles on the Road. 1-A Qualitative Gas Chromotography/Mass Spectrometry Survey", Environ. Sci. Technol., Vol. 16, No. 5, 1982.

27. Hampton, C.V., W.R. Pierson, D. Scheutzie, and T.M. Harvey, "Hydrocarbon Gases Emitted from Vehicles on the Road. 2. Determination of Emission Rates from Diesel and Spark-Ignition Vehicles", Environ. Sci. Technol., Vol. 17, No. 12, 1983.

28. Pierson, W.R., W.W. Brachaczek, R.H. Hammerle, D.E. McKee, and J.W. Butler, "Sulfate Emissions from Vehicles on the Road", Journal of the Air Pollution Control Association, 28, 123, 1978.

29. Pierson, W.R., R.A. Gorse, A.C. Szkarlat, W.W. Brachazek, S.M. Japar, F.S.C. Lee, R.B. Zweidinger, and L.D. Claxton, "Mutagenicity and Chemical Characteristics of Carbonaceous Particulate Matter from Vehicles on the Road", Environ. Sci. Technol., 17, 31, 1983.

30. Pierson, W.R., W.W. Brachaczek, and D.E. McKee, "Sulfate Emissions from Catalyst-Equipped Automobiles on the Highway", APCA Journal, 29, 255, 1979.

31. Pierson, W.R., "Particulate Organic Matter and Total Carbon from Vehicles on the Road", Tech. Report No. Sr-80-34, March, 1980.

32. Pierson, W.R., and W.W. Brachaczek, "Particulate Matter Associated with Vehicles on the Road", Society of Automotive Engineers, Inc., #760039.

33. Pierson, W.R., and W.W. Brachaczek, "In Traffic Measurement of Airborne Tire-Wear Particulate Debris", Journal of the Air Pollution Control Association, Vol. 25, No. 4, April, 1975.

34. Ondov, J.M., "A Study of Trace Elements on Particulates from Motor Vehicles", Diss. Abstr. Int., B36:147, 1979.

35. Ondov, J.M., W.H. Zoller, and G.E. Gordon, "Trace Element Emissions on Aerosols from Motor Vehicles", Environ. Sci. Technol., 16:318-328, 1981.

36. Pierson, W.R., and W.W. Brachaczek, "Particulate Matter Associated with Vehicles on the Road", Soc. Automotive Engineers Trans., 85, 209, report no. 760039, 1976.

37. Pierson, W.R., and D.E. McKee, "Light Scattering by Particulate Emissions from Vehicles on the Road", J. Air Pollution Control Assoc., 28, 604, 1978.

38. Pierson, W.R., D.E. McKee, W.W. Brachaczek, and J.W. Butler, J. Air Pollution Control Assoc., 28, 692, 1978.

39. Model 244, Sierra Instruments dichotomous virtual impactor.

40. A SCENES audit of mass determination was conducted September 15, 1986, by Mr. C. Lanane of ER&T. The results were reported to EPRI on September 22, 1986, with a recommendation to continue with current procedures.

41. NEA, Inc., "California Desert Particle Trace Element Analysis Study", 1986. The analysis of eight hundred filters that had previously been analyzed by PIXE at U.C. Davis. Sponsor: Western Oil and Gas Association. Data processed by Mr. Mike McGowan, U.S. EPA, MD 77B, Research Triangle Park, NC 27711.

42. EPA audit of XRF analysis results, February, 1985, Ms. L. Porter, U.S. EPA, MD 77B, Research Triangle Park, NC 27711.

43. Blanchard, D.C., and A.H. Woodcock, "The Production, Concentration, and Verticle Distribution of the Sea-Salt Aerosol", Ann. N.Y. Acad. Sci., 1979.

44. Pierson, W.R., and W.W. Brachaczek, "Airborne Particulate Debris from Rubber Tires", Rubber Chemistry and Technology, 47, 1275, 1974.

45. Pierson, W.R., and W.W. Brachaczek, "In-Traffic Measurement of Airborne Tire-Wear Particle Debris", J. Air Pollution Control Assoc., 25, 404, 1975.

46. Cadle, S.H., and R.L. Williams, "Gas and Particle Emissions from Automobile Tires in Laboratory and Field Studies", J. Air Pollution Control Assoc., 28, 502, 1978.

47. Cardina, J.A., "Particle Size Determination of Tire-Tread Rubber in Atmospheric Dusts", Rubber Chem. Technol., 47, 1005, 1974.

48. Dannis, M.C., "Rubber Dust from the Normal Wear of Tires", Rubber Chem. and Technol., 47, 1011, 1974.

49. Environmental Protection Agency, "Compilation of Air Pollutant Emissions Factors", AP-42, fourth edition, Sept. 1985, Appendix L, "Size Specific Total Particulate Emission Factors for Mobile Sources", August, 1985.

50. Muhlbaier, J.L., and R.L. Williams, "Characterization of Asbestos Emissions from Brakes", GMR-3435, General Motors Research Laboratories, Warren, MI, 1980.

51. Cha, S., P. Carter, and R.L. Bradow, "Simulation of Automobile Brake Wear Dynamics and Estimation of Emissions", Society of Automotive Engineers technical paper 831036. Passenger Car Meeting, Dearborn, MI, June 6-9, 1983, Warrendale, PA.

PART II

OTHER DIRECT PROFILE MEASUREMENTS

EXECUTIVE SUMMARY

Source profiles were developed for other high priority sources defined in the PM_{10} source profile development plan. These sources included soil and road dust, construction, rock crusher, coke calciner, and petroleum fluid catalytic ~~converter~~ *cracker*. Soil and road dust samples were collected from forty-one streets, parking lots, and vacant lots around each of the monitoring sites. These dust samples, along with bulk samples from construction sources, a rock crusher and coke calciner, were aerosolized in the laboratory and sampled with a dichotomous sampler. The catalytic ~~converter~~ *cracker* was sampled with a size-segregating dilution sampler.

1.0 INTRODUCTION

The PM_{10} source profile development plan (1) recommended the collection and analysis of emission samples from the four highest priority source categories; i.e.

- on-road motor vehicles

- soil and road dust

- construction and demolition, and

- petroleum refining (catalytic crackers)

Emissions from two other source categories of special interest, coke calcining, and rock crushing, were also designated to be characterized. Characterization of on-road motor vehicles was discussed in Part I of this volume. The methods used to develop source profiles for these other sources and the results are discussed in this part of the report.

2.0 EXPERIMENTAL

2.1 Sample Collection

2.1.1 Paved Road Dust

Samples of aerosolizable surface dust on paved roads were collected using a high volume vacuum motor with an 8 inch by 10 inch filter holder to which a vacuum hose and brush was attached. The street surface was brushed with the vacuum brush attachment, and the entrained dust particles collected on a glass fiber filter. Sampling was continued until a thick (> 1/4 inch) deposit had accumulated on the filter. The deposit was then placed in a plastic bag for return to the laboratory for processing.

Paved road dust samples were collected predominantly from the center of the curb side lane. The Artesia Freeway sample

was collected from the middle of a curb side lane from which traffic had been diverted for a few hours. The Pasadena Freeway sample was collected from the middle of an on-ramp from which traffic had been diverted.

2.1.2 Unpaved Roads, Soils, and Construction

Aerosolizable dust samples from unpaved roads, soil surfaces, and around construction sites were obtained by brushing or scraping the surface dust into a dust pan which was then transferred to a plastic bag.

2.1.3 Rock Crusher

Dust that had settled on and around a rock crusher was scraped and brushed into a plastic bag.

2.1.4 Coke Calciner

Baghouse catch dust was sampled by plant operating personnel and shipped to NEA for processing.

2.1.5 Petroleum Catalytic ~~Converter~~ Cracker

A size-selective dilution sampler, as illustrated in Figure 1, was used to collect fine (< 2.5 μm) and coarse (2.5-10 μm) particles simultaneously on Teflon and quartz fiber filters with two dichotomous virtual impactors. The sampler probe and dilution chamber are all stainless steel. In its normal operation, a pressure difference between the chamber and the stack is established by varying the flow rates of the inlet and outlet blowers. Particles less than 10 μm in diameter are drawn into the dilution chamber isokinetically through a cyclone and heated transfer tube or probe. Filtered dilution air is mixed with the stack aerosol in the dilution chamber. This cools and dilutes the stack aerosol simulating the condensation and evaporation in a

92

Pressure Sensing Port

Velocity Sensing Port

Relative Humidity Port

Temperature Sensing Port

Exhaust Air
Filter Holder

Variable Diameter
Inlet Tubes

Dichotomous Virtual
Impactor Sampling Heads

4 inch Diameter
Residence Chamber

Dilution Air
Filter Holder

Dilution Air
Blending Module

Instrument Module

Simplified Front
View of Diffusion
Flow Plate

Particle Pre-separator

Pilot Tubes

Inlet Nozzle

Flow Transducer

Flow Plate

Heat Tape

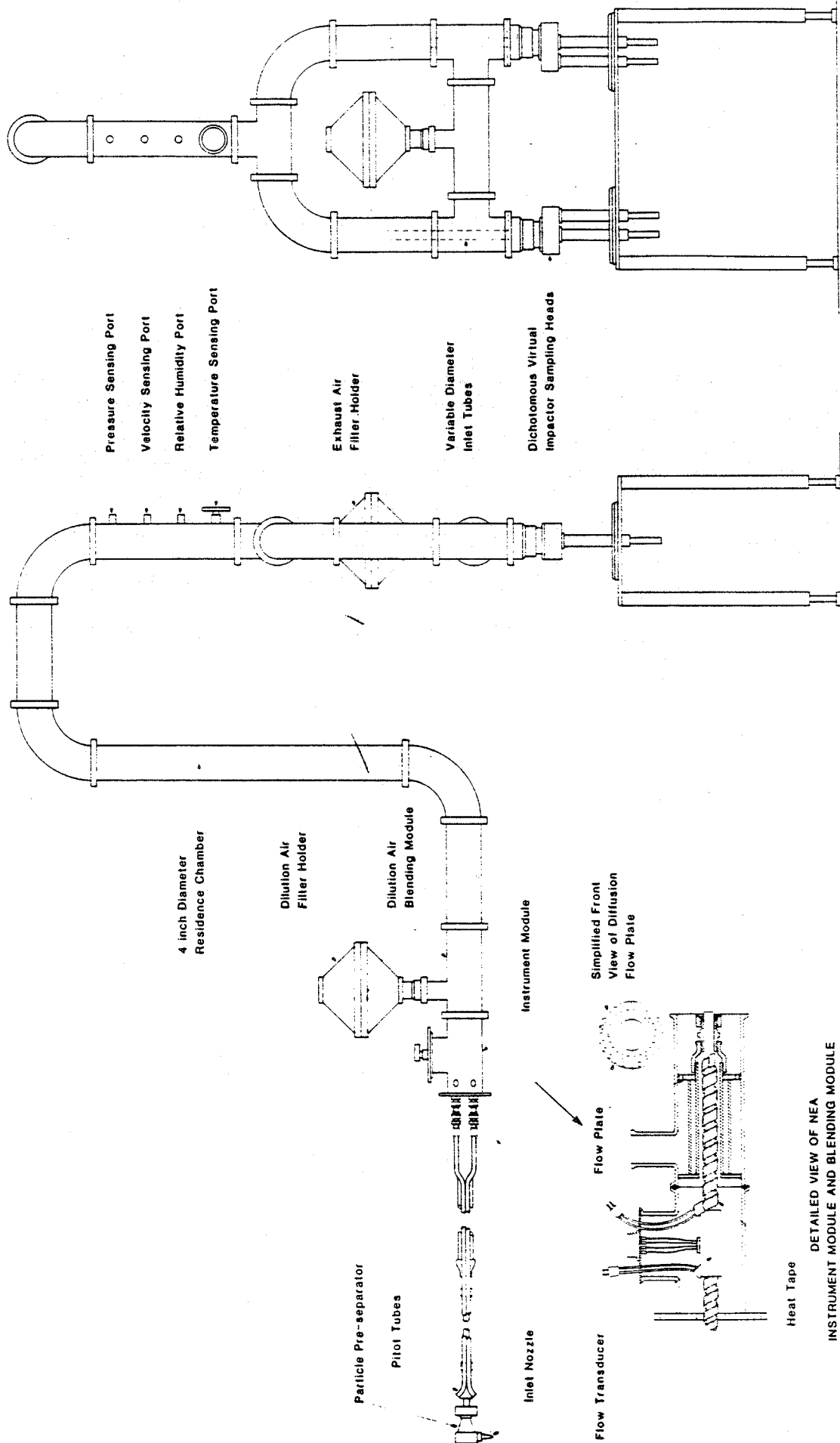DETAILED VIEW OF NEA
INSTRUMENT MODULE AND BLENDING MODULE

Figure 1. Schematic illustration of NEA's size-segregating dilution sampler used to collect samples from the fluid catalytic cracker.

93

plume. The cooled aerosol is then sampled with two virtual impactor dichotomous samplers. In this way, size selective samples are collected that minimize modifications in emission chemistry due to evaporation, condensation, and sedimentation during transport. In addition, the filter samples can be analyzed with analytical methods similar to those used for ambient filters, thus minimizing systematic effects due to analytical or sampling differences.

2.2 Dust Sample Preparation and Aerosolization

Samples collected on filters were gently shaken to separate the dust from the filter. This separated dust was then processed the same as the other bulk dust samples. That is, large rocks, particles, and other debris were separated from the aerosolizable dust by sieving the sample through a 400 mesh Tyler screen (38 μm). The resulting dust samples were either aerosolized directly or first combined in specific proportions with other sieved dust samples and resieved to mix this composite sample before aerosolization.

These fine powder-like samples were aerosolized in a dust chamber and sampled on both Teflon and quartz fiber filters using a Sierra dichotomous virtual impactor with a 10 μm inlet. In this procedure, small quantities of dust were aerosolized, after which the coarse particle filter was weighed. This procedure was continued until between 300 and 600 μg/cm^2 of deposit had been accumulated. The fine particle filter was then weighed and the fine to coarse particle ratio determined.

Because only about 5 to 10% of the PM$_{10}$ dust consists of fine particles, the analytical sensitivity for the fine particle fraction would not be comparable to the coarse particle fraction. To improve the analytical sensitivity of the fine particle fraction, the deposit area was collimated from the normal 6.6 cm^2 area to an area of 2.2 cm^2. In addition, after an adequate coarse particle filter deposit mass had been attained, it was replaced with a scrap

coarse particle filter and the aerosolization continued until a similar deposit mass per cm^2 was obtained for the fine particle filter.

2.3 Filter Analysis

The filter samples collected from the fluid catalytic cracker and laboratory dust aerosolization were analyzed for deposit mass, organic and elemental carbon, and inorganic elemental content by the procedures described in Section 3.3 of Part I of this report.

2.4 Sample Description

Road dust and soil samples were collected from forty-one streets, parking, and vacant lots around each of the monitoring sites.

One paved road dust sample was collected from a major street near each ambient monitoring site. Samples from other paved streets in the local area around each site were also collected but were combined after sieving to form a composite paved road dust sample for each site. Soil and unpaved road dust samples in the area of the Rubidoux monitoring site were also sampled. In addition, two freeway dust samples, two tunnel dust samples, and three construction dust samples were collected.

The sandblasting and plastering sample was collected at a building site where a crew was sandblasting concrete structures. The building was under construction and located in the industrial complex west of the Hawthorne monitoring site. Dust samples were collected from deposits which had accumulated around the base of the building which was assumed to be from the sandblasting of concrete, as well as activities inside the building such as wallboarding and plastering.

Other samples of construction emissions consisted of excavation and grading samples from a highway construction site located near where Interstate 405 crosses over El Segundo Boulevard. The excavation sample consisted of soil collected from various areas around the construction site and the grading sample was collected from a haul road at the construction site.

The location where these samples were collected and how they were combined to form composite samples are summarized in Table 1.

The rock crusher dust was collected from the Livingston Graham plant in Irwindale.

The coke calciner baghouse dust was supplied by ARCO CQC Kiln, Inc. in Wilmington. The baghouse dust is their flue gas desulfurization ash from the coking operating. In this process, "green" coke, obtained from the ARCO Refinery, is calcined in a kiln-burner unit. The coke purification process consists of heating the raw coke to a temperature below its fusion point to remove volatile materials. The emissions from the kiln are further treated in an afterburner-like device designated as a pyroscrubber. The hot pyroscrubber exhaust is passed through a waste-heat boiler to extract heat and produce steam for plant use. The effluent is then desulfurized in a scrubber using calcium hydroxide solution. The exhaust from the scrubber is then vented through a baghouse to control particulate emissions. It is the baghouse dust that was analyzed in this study.

The fluid catalytic cracker (FCC) sampled was located at the Chevron U.S.A., Inc. El Segundo Refinery. The number 39 FCC was selected for sampling at the refinery. It is similar to the other FCC units used by Chevron. Emissions from the catalyst are typically cleaned from the exhaust with an electrostatic precipitator (ESP) and the catalyst periodically recovered from the ESP. In this particular unit, ammonia was being added to compensate for one of the ESP's that was nonfunctional at the time of our sampling.

Table 1

DESCRIPTION OF ROAD DUST, SOIL, CONSTRUCTION, AND INDUSTRIAL SAMPLES FOR RESUSPENSION

Region No.	Mnemonic	Profile Name	Sample Description
1	PRDLBB	Long Beach Blvd.	Long Beach A; Long Beach Blvd. (100%)
1	PRLBSC	Long Beach Sample Composite	Long Beach B; E. Wardlow (17%), Atlantic (17%), Elm St. (17%), Bixby (17%), 36th St. (17%), 37th St. (17%)
2	PRDLCB	La Cienega Blvd.	Hawthorne A; La Cienega Blvd. (100%)
2	PRDHSC	Hawthorne Sample Composite	Hawthorne B; 120th St. (20%), Isis St. (10%), 119th St. (10%), Aviation Blvd. (30%), El Segundo (30%)
3	PRDVB	Victory Blvd.	Burbank A; Victory Blvd (100%)
3	PRDBSC	Burbank Sample Composite	Burbank B; Orange Grove (20%), Olive St. (20%), Palm St. (20%), Lake St. (20%), Magnolia (20%)
4	PRDNMS	North Main Street	Los Angeles A; N. Main St. (100%)
4	PRLASC	Los Angeles Sample Composite	Los Angeles B; Wilhardt (25%), N. Spring Rd. (25%), Leroy St. (25%), Alhambra St. (25%)
5	PRDSHB	South Harbor Blvd.	Anaheim A; South Harbor Blvd. (100%)
5	PRDASC	Anaheim Sample Composite	Anaheim B; Vermont St. (50%), Ball Rd. (25%), Clifton Ave. (12.5%), Cambridge St. (12.5%)
6	PRDRSC	Riverside Sample Composite	Riverside A; Mission Blvd. (45%), Riverview Dr. (30%), LaRue (5%), Renee St. (5%), Patty St. (5%), Highway 60 (10%)
4	FRDPAS	Pasadena, 110	L.A. Freeway A; Pasadena Freeway, Hwy. 110 on-ramp (100%)
1	FRDART	Artesia, 91	L.A. Freeway B; Artesia Freeway, Hwy. 91 right traffic lane (100%)
2	PRSTC	Sepulveda Tunnel	Sepulveda Tunnel A; Southbound tunnel samples, I (50%), II (50%)
6	UPRDRS	Riverside Sample Composite	Riverside B; Mission (15%), Janet (15%), LaRue (30%), Riverview (15%), County (25%)
2	CDEXCA	Excavation, I405/ El Segundo	L.A. Construction B; excavation soil sample from I405 access ramp (100%)

Table 1

-Continued-

Region No.	Mnemonic	Profile Name	Sample Description
2	CDEXHL	Excavation, Haul Road, I405/ES	L.A. Construction A; sample from haul roads on I405 excavation (100%)
2	CDSAPL	Sandblasting and plastering	L.A. Construction C; building construction Grand Ave. Business Park (100%)
1	PRCCSC	Coke calcining, SCAB, 1987	L.A. Industrial B; ARCO Coke Calciner Flue gas desulfurization ash (100%)
3	CDRKCR	Rock crushing, SCAB 1987	L.A. Industrial A; Livingston Graham Rock Crusher, Irwindale (100%)

The filter samples collected at the FCC are listed in Table 2. The mass loadings were all low. The X-ray fluorescence analysis results for each filter are listed in Appendix T, and the average profile is listed in the source library.

2.5 Filter Deposit Mass and Fine to Coarse Ratios

The filter samples obtained during the dust aerosolization and sampling step are listed in Table 3 for each dust sample. Also listed in this table are the final deposit mass on each filter and the intermediate fine to coarse ratio. The intermediate fine to coarse ratios were determined after an adequate mass loading was obtained on the first coarse particle filter.

3.0 RESULTS AND DISCUSSION

3.1 General Chemical Composition

The detailed chemical analysis results for each filter are presented in the source profile library in Volume II of this report. They are in the same format as described in Part I of this volume.

About 40% to 50% of the bulk dust mass is typically explained by the species measured. The percent mass explained is increased to about 90 to 100% when unmeasured species such as O, N, and H associated with the organic carbon compounds, the unmeasured Na and Mg, each of which typically represent about 2% of the mass, and the oxygen associated with all of the inorganic species are taken into account.

A much smaller portion of the FCC mass is explained by the measured species. Oxygen associated with species such as Al and Si can account for some of the unexplained mass, but the species associated with the rest of the mass is unknown.

Table 2

CHARACTERISTICS OF THE FILTER SAMPLES
COLLECTED FROM THE CHEVRON FLUID CATALYTIC CRACKER

Run No.	Filter ID	Filter Media	Size	Start Date	Start Time	Duration (Hours)	Deposit Mass(µg)
1	MI073	Teflon	F	12-10-86	1553	1.04	37
	MI074	Teflon	C			1.04	41
	MI216	Quartz	C			1.04	
	MI217	Quartz	F			1.04	
2	MI075	Teflon	F	12-11-86	0815	2.08	62
	MI076	Teflon	C			2.08	59
	MI218	Quartz	C			2.09	
	MI219	Quartz	F			2.09	
3	MI077	Teflon	F	12-11-86	1050	2.04	61
	MI078	Teflon	C			2.04	46
	MI220	Quartz	C			2.04	
	MI221	Quartz	F			2.04	
4	MI079	Teflon	F	12-11-86	1306	3.51	92
	MI080	Teflon	C			3.51	69
	MI222	Quartz	C			3.51	
	MI223	Quartz	F			3.51	

Table 3

AEROSOLIZED DUST FILTER IDENTIFICATION,
DEPOSIT MASS, AND FINE/COARSE RATIOS

Source Category	Filter ID	Particle Size	Final Deposit Mass (μg)	Intermediate F/C Ratio
Long Beach Blvd.	MI903	F	168	0.027
	MI902	C	2346	
Long Beach Composite	MI905	F	165	0.015
	MI904	C	2551	
La Cienega Blvd.	MJ193	F	194	b
	MJ194	C	3081	
Hawthorne Composite	MJ195	F	163	b
	MJ196	C	2720	
Victory Blvd.	MI907	F	150	0.019
	MI906	C	3931	
Burbank Composite	MI909	F	152	0.013
	MI908	C	2510	
North Main Street	MI911	F	150	0.010
	MI910	C	2903	
Los Angeles Composite	MI913	F	113	0.008
	MI912	C	2831	
South Harbor Blvd.	MI915	F	134	0.006
	MI914	C	2424	
Anaheim Composite	MI917	F	249	0.018
	MI916	C	4047	
Riverside Composite	MI899	F	246	0.040
	MI898	C	3102	
Sepulveda Tunnel	MI919	F	169	0.015
	MI918	C	2643	
Pasadena, 110	MJ199	F	353	b
	MJ200	C	2853	
Artesia, 91	MJ201	F	190	0.035
	MJ202	C	2518	
Riverside Soil	MI901	F	210	b
	MI900	C	3828	
Excavation, I405/ El Segundo	MJ205	F	157	0.020
	MJ206	C	2140	
Excavation, Haul Roads, I405/ES	MJ203	F	150	0.020
	MJ204	C	3387	
Sandblasting and Plastering	MJ207	F	408	0.068
	MJ208	C	5994	

Table 3

-Continued-

Source Category	Filter ID	Particle Size	Final Deposit Mass (μg)	Intermediate F/C Ratio
Coke Calcining, SCAB, 1987	MI101	F	291	b
	MI102	C	2894	
Rock Crushing, SCAB, 1987	MJ197	F	308	b
	MJ198	C	2998	

a. Additional material is loaded onto the fine fraction after the coarse fraction has reached desired deposit range.

b. No intermediate ratio information available.

3.2 Source Profiles

3.2.1 Fluid Catalytic Cracker

Petroleum refining operations are significant sources of particulate emissions in the SCAB, and they are one of the largest point sources in the vicinity of the Hawthorne and Long Beach sites. Although there is a wide range of source types within this source category, FCC's were thought to have one of the more characteristic emissions in which rare earth elements are released.

The FCC source profiles resulting from our sampling and analysis are presented in the source library. The fine particle composition is compared with other measurements in Table 4. The spectrographic analysis profile is the average of about eight routine semi-quantitative analysis of different FCC units in the SCAB (2). The Philadelphia profile is based on the analysis of about four samples by X-ray fluorescence and neutron activation analysis (3). The Cubatao profile represents the analysis of resuspended, recycled catalyst (4).

The profile from this work was developed from the analysis of three replicate samples collected over a period of twenty-four hours. The emissions from the Chevron unit were so low that even after four hours of sampling with a dilution ratio of about 10:1, only 150 μg had been collected. The deposit masses are close to the uncertainty of about 10 μg for the determination of a net deposit. The fine to coarse ratio was much lower than had been previously measured.

There was excellent agreement between the fine and coarse samples collected in this work, but there was substantial variability with size in the Philadelphia and Cubatao profiles. The most abundant species in all the profiles are Al and Si. The next most abundant species was S, followed by Ce, Ti, La, and Nd.

103

Table 4

COMPARISON OF FLUID CATALYTIC CRACKER SOURCE PROFILES
FOR PERCENT COMPOSITION (FINE FRACTION)

Species	Spectrographic[2] (n=8)	Phildelphia[3] (n=?)	Cubatao[4] (n=1)	This Work (n=3)
Na	1.75 ± 1.68	.36 ± .04		
Mg	.151 ± .135			
Al	2.75 ± 2.48	6.50 ± 1.10	21.41 ± 2.14	18.38 ± 2.43
Si	5.11 ± 6.12	9.80 ± 1.30	43.46 ± 4.35	17.85 ± 2.48
P		.16 ± .03	.25 ± .05	.042 ± .024
S		4.20 ± .50	.32 ± .08	1.65 ± .38
Cl			.059 ± .028	.25 ± .07
K		.031 ± .005	.15 ± .02	.18 ± .02
Ca	.46 ± .27	.030 ± .004	.25 ± .02	.16 ± .02
Sc		.000 ± .000		
Ti	0.09 ± 0.13	.35 ± .09	1.00 ± .10	.80 ± .09
V	.009 ± .009	.023 ± .007	.44 ± .04	< .20
Cr	0.25 ± 0.55	.006 ± .001	.11 ± .01	< .08
Mn	.042 ± .043	.001 ± .000	.065 ± .008	< .03
Fe	1.95 ± 3.92	.20 ± .03	.96 ± .10	.69 ± .11
Co	.009 ± .003	.001 ± .000		
Ni	0.42 ± 0.88	.022 ± .003	.25 ± .03	.017 ± .010
Cu	.019 ± .022	.001 ± .001	.047 ± .009	.001 ± .002
Zn	.20 ± .15	.002 ± .001	.040 ± .007	.012 ± .007
Ga			< .005	.003 ± .002
As			< .017	.010 ± .007
Se		.001 ± .000	< .004	.006 ± .002
Br		.001 ± .000	.015 ± .006	.003 ± .004
Rb			< .006	< .002
Sr		.004 ± .001	.017 ± .008	< .003
Y			.003 ± .009	< .004
Zr	.005 ± .003	.012 ± .004	< .040	< .015
Mo	.157 ± .208		< .030	< .010
Ag	.003 ± .003		< .041	< .013
Cd	.119 ± .153		.011 ± .055	< .017
In			.098 ± .061	< .021
Sn	.098 ± .175	.005 ± .002	.072 ± .074	< .025
Sb		.001 ± .000	.17 ± .13	< .057
Ba		.032 ± .004	< .35	< .105
La	.177 ± .166	.31 ± .04	.20 ± .53	.43 ± .32
Ce		.25 ± .04		1.36 ± .12
Nd	.177 ± .210	.17 ± .02		.40 ± .06
Au	.002 ± .001			
Hg			.017 ± .008	.001 ± .002
Sm		0.16 ± .002		
Pb	.126 ± .185	.009 ± .002	.15 ± .02	< .006

Although not all of the mass is necessarily explained in each profile, it is assumed that the unexplained mass is associated with species not measured. This is supported by the loss on ignition values reported by the spectrographic analysis, which ranged from 33% to 93%. The enrichment of La and rare earth elements was common for all of the profiles, but there was considerable variation in the rare earth ratios relative to La. Although these rare earth elements had originally been thought to be reasonably unique indicators for this source category and may still be, the observation of Ce in the tailpipe exhaust of a catalyst equipped vehicle suggests that similar species may be emitted by this latter interfering source. The large variability in the relative composition of the rare earth elements within the FCC category, however, suggests the possibility of distinguishing individual sources within this source category if a similar degree of variability between the relative rare earth concentrations is observed.

3.2.2 Coke Calciner

The coke calciner profile consists almost exclusively of S and Ca. The S concentration of about 16% and Ca concentration of about 27% is consistent with the analysis reported by ARCO and listed below:

	%
Calcium sulfate dehydrate	5
Calcium sulfate hemihydrate	16
Calcium sulfate anhydrous	10
Calcium sulfite	18
Calcium hydroxide	9
Calcium carbonate	30
Carbon	10
Ash	2
Total	100
Ca	31
S	11.3

105

The carbon associated with this source is essentially all carbonate carbon. Very little unburned carbon passes through the pyro-scrubber. The baghouse catch that was aerosolized and analyzed to develop this profile was essentially white. It is felt that this baghouse catch should be representative of the particulate emissions chemistry of this source.

3.2.3 Rock Crusher

The rock crusher profile developed as part of this study and a rock crusher profile developed in Portland, Oregon, in 1978, are both listed in the library. The profiles are quite similar with each containing about 29% Si. The profile reported for the Livingston Graham rock crusher is as expected from the mineralogy reported by the company which indicated 43% feldspartic, 50% amphibolic gneiss, with 7% other minor mineralogical species.

3.2.4 Construction

A single composite construction-demolition profile is not listed in the source profile library. Instead, profiles for individual activities within this category are provided. A composite profile for the entire category would require knowledge about the relative emission rates which are expected to vary considerably over the airshed.

The construction and demolition emissions source category is one of the largest in the SCAB, representing 27% of the 1983 emissions inventory, or 175 tons per day (TPD). This general category includes the construction and demolition of a wide range of structures such as high rise buildings, industrial and manufacturing facilities, residential subdivisions, and roads. The emissions, subdivided by the type of structure being constructed or demolished are listed below:

Residential	57.1	tons per day
Industrial	29.7	
Government	28.0	
Roads	21.9	
Institutional	19.3	
Commercial	19.0	
Total	175.0	tons per day

The particulate sources that would have to be controlled if the emissions from this general source category are to be reduced include such construction and demolition activities as:

- Excavation, grading, and movement of soil;

- Activities associated with soil removal such as track out, spillage on roads, and wind entrainment from trucks during haulage;

- Wind entrainment from exposed soils;

- Welding of reinforcing steel, steel buildings;

- Concrete and steel sanding, sand blasting;

- Roofing and stripping of old roofs;

- Plastering, wallboard, fiber glass, and general materials handling during construction and demolition of structures and roads;

- Demolition and removal of materials used in the construction of roads and buildings;

- Asphalt paving.

Of most interest in receptor modeling are the chemical and physical properties of the emissions from these activities. The activities, for example, can be separated into two major coarse particle categories and two fine particle categories as follows:

Coarse Particles

- Silicon-rich soil emissions such as excavation, grading, hauling and spilling soil, wind entrainment of soil from exposed areas, and

- Calcium-rich emissions from activities like concrete
  spills, Portland cement handling, concrete sanding,
  plastering, construction with gypsum products,
  demolition of walls constructed of calcium rich
  materials.

Fine Particles

- Iron-rich emissions from such sources as welding, and

- Carbon-rich emissions from roofing, asphalt paving, etc.

Although the emission figures are not available in these source
groupings, the coarse particle emissions are expected to account for
over 90% of the mass and the silicon-rich coarse particles probably
are responsible for more of the coarse particle mass than the
calcium-rich emissions.

The silicon-rich sources will be difficult to resolve
from the soil and road dust category, simply on the basis of
chemical characteristics and particle size. The calcium-rich
emissions, however, are likely to be resolvable from the soil and
road dust category. This category is represented by the first three
source profiles listed in the construction and demolition category.
Although the fine particle sources listed and others associated with
this category may be a small fraction of the total category, they
may influence the ambient fine particle chemistry at a local site on
any given day. Roofing and asphalt paving, for example, are
activities not necessarily correlated in time with excavation or
concrete work. A welding profile from a 1973 uranium mine study is
included to represent this activity. Although the emissions from
the construction or demolition of a high rise building were not
collected in this study, there is the possibility of developing such
a profile from ambient data in Phoenix, Arizona, where a high rise
building was constructed next door to one of our monitoring sites.

3.2.5 Paved and Unpaved Surfaces and Roads

The concentrations of selected elements, OC and EC in paved and unpaved surfaces and roads are listed in the Source Profiles in Volume II. A comparison of these profiles shows the highest concentrations of inorganic species such as Al and Si were measured in Riverside samples, while the lowest concentrations were measured in dust samples collected in downtown Los Angeles. In contrast, the concentration of OC and EC was lowest in the Riverside dust and highest in the downtown Los Angeles dust. This is as expected, since one of the main components in road dust is soil, which is the primary source of Al and Si. The ~~concentration~~ Percent contribution of soil, and therefore, Al and Si, is expected to decrease as other source contributions such as tire wear, etc., increase. The concentration of Zn also varies in a manner similar to carbon, with the highest concentrations being measured in downtown Los Angeles and on the Pasadena Freeway, and the lowest concentration being measured in the Riverside samples and the La Cienega Blvd. paved road dust samples.

The La Cienega Blvd. samples are unusual because they would be expected to have a higher concentration of Zn and organic carbon due to all the traffic in this area and the generally small amount of unpaved surfaces. However, a large scale construction project was being conducted within a block of the area where the sample was collected, and soil track out was substantial. Although the sample was collected in the middle of the road, there was a noticeable amount of crustal material on La Cienega Blvd. and other streets around the Hawthorne monitoring site.

4.0 REFERENCES

1. NEA, Inc., "PM$_{10}$ Source Profile Library Development Plan for the South Coast Air Basin", final report to the South Coast Air Quality Management District, July 8, 1986.

2. Spectrographic Analysis Results submitted to the South Coast Air Quality Management District.

3. Olmez, I., A.E. Sheffield, G.E. Gordon, J.E. Houck, L.C. Pritchett, J.A. Cooper, T.G. Dzubay, and R.L. Bennett, "Composition of Particles from Selected Sources in Philadelphia for Receptor Modeling Applications", to be published in the Journal of Air Pollution Control Assoc., 1987.

4. Miller, E.A., J.A. Cooper, C.A. Frazier, and L.C. Pritchett, "Cubatao Aerosol Source Apportionment Study", final report to CETESB, Sao Paulo, Brazil, from NEA, Inc., Beaverton, OR, March, 1985.